
The role of in situ stress in determining hydraulic connectivity in a fractured rock aquifer (Australia)

Luke Mortimer · Adnan Aydin · Craig T. Simmons ·
Graham Heinson · Andrew J. Love

Abstract Fracture network connectivity is a spatially variable property that is difficult to quantify from standard hydrogeological datasets. This critical property is related to the distributions of fracture density, orientation, dimensions, intersections, apertures and roughness. These features that determine the inherent connectivity of a fracture network can be modified by secondary processes including weathering, uplift and unloading and other mechanisms that lead to fracture deformation in response to in situ stress. This study focussed on a fractured rock aquifer in the Clare Valley, South Australia, and found that fracture network connectivity could be discriminated from several geological, geophysical and hydrogeological field datasets at various scales including single well and local- to regional-scale data. Representative hydromechanical models of the field site were not only consistent with field observations but also highlighted the strong influence of in situ stress in determining the distribution of fracture hydraulic apertures and the formation of hydraulic chokes that impede fluid flow. The results of this multi-disciplinary investigation support the notion that the hydraulic conductivity of a fracture network is limited to the least hydraulically conductive interconnected fractures, which imposes a physical limit on the bulk hydraulic conductivity of a fractured rock aquifer.

Keywords Fractured rocks · Groundwater hydraulics · Hydromechanical model · In situ stress · Australia

Introduction

Groundwater flow within fractured rock aquifers is dominantly controlled by fracture density, length, geometry, connectivity, infill (e.g. mineralisation, detrital clays), weathering and the effects of the present-day in situ stress field. Of these seven key parameters, connectivity is possibly the most difficult parameter to identify in the field largely as it is a subjective term that can only be quantified via indirect measurements (NRC 1996). The term connectivity describes the relative amount of interconnection between finite fractures within a fracture network with the implication that higher degrees of fracture interconnection results in higher overall rock-mass permeability. An understanding of the concept of connectivity within a fractured rock aquifer is important because although it is directly linked to fracture properties such as fracture density, orientation, length and aperture, it is an independent factor that has a significant impact on fracture network hydraulics. For example, a densely fractured rock mass may still have a low connectivity and permeability if the fractures are of a similar orientation with few intersections.

The closest analogy to the term connectivity is the concept of percolation as defined in percolation theory, which is the study of random networks of conductors and the probability that random fractures are connected and conductive (NRC 1996). Percolation theory is used to estimate the critical fracture density required for an infinite number of connected and conductive fracture clusters or “percolation” (NRC 1996). Below this critical density threshold there are only finite-sized clusters of connected fractures or no percolation (NRC 1996). However, the basis for percolation theory and hydraulic connectivity is scale-dependent and will vary with the scale of investigation. For example, Long and Witherspoon (1985) found that large-scale samples of a well-connected fracture network may percolate but a smaller-scale sample of the same network may not. The key is whether the scale of measurement is sufficient to capture a statistically representative sample of the fracture network, assuming that

Received: 6 July 2010 / Accepted: 30 June 2011
Published online: 19 July 2011

© Springer-Verlag 2011

L. Mortimer (✉) · C. T. Simmons · A. J. Love
School of the Environment and National Centre for Groundwater
Research and Training,
Flinders University,
G.P.O. Box 2100, Adelaide, South Australia 5100, Australia
e-mail: luke.mortimer@flinders.edu.au
Tel.: +61-3-98277740
Fax: +61-8-82015635

A. Aydin
Department of Geology and Geological Engineering,
University of Mississippi,
PO Box 1848, University, MS 38677, USA

G. Heinson
School of Earth and Environmental Sciences,
University of Adelaide,
Adelaide, South Australia 5005, Australia

the fractured rock mass is homogeneous (Long et al. 1982; Long and Witherspoon 1985).

There are many numerical modelling studies concerned with the determination of connectivity within fractured rock masses. These studies cover issues such as site characterisation and model validation, scale dependence and scale effects of fracture-network permeability, relationships between permeability and fracture parameters such as density, length and aperture distributions as well as appropriate modelling methodologies for applications such as flow and contaminant transport at fractured rock sites (e.g. Bour and Davy 1998; Davy et al. 2006; de Dreuzy et al. 2001; Long et al. 1982; Long and Witherspoon 1985; Hsieh 1998; Odling et al. 1997; Renshaw 1996, 1999; Wellman and Poeter 2006). There are also numerous field-based studies, which have inferred the existence of hydraulic connections between multiple boreholes within a fractured-rock aquifer site as detected via direct borehole hydraulic testing (e.g. Cook 2003; NRC 1996; Paillet 1993; Shapiro et al. 2007). However, these particular field-based methods largely rely on detecting interference/anomalies within observation wells, which through their own establishment may alter the natural hydraulics of the system and introduce unnatural connections within the aquifer (Paillet 1993). To avoid these unnatural connections techniques that test an aquifer without observation wells or isolate discrete well intervals (e.g. inflatable packers) are required (Paillet 1993; Shapiro et al. 2007). However, in field-based studies, the identification or more often the inference of processes that determine sub-surface fracture network connectivity is complex and problematic and strongly scale-dependent. Therefore, the key to understanding fracture network connectivity is observation over a wide (metre to kilometre) scale range yet this is rarely achieved for practicality and cost reasons.

Due to the inherent heterogeneous nature of fractured rock aquifers, field-based studies relating to fracture network connectivity require that the structural and hydraulic nature of fractured rock aquifers be characterised through a multi-disciplinary approach that incorporates several methodologies including hydrogeochemistry, geological mapping and borehole hydraulic and geophysical testing. One good example of this type of multi-disciplinary approach is presented by Shapiro et al. (2007) which used a wide range of field and hydrogeological modelling techniques to characterise groundwater flow and solute transport over metre to kilometre scales in fractured crystalline rocks at the Mirror Lake site, New Hampshire. For example, Shapiro et al. (2007) measured the transmissivity of discrete individual and closely spaced fracture sets within 3–5 m wide packer-isolated sections of single wells and found that these varied by six orders of magnitude (10^{-4} – 10^{-10} $\text{m}^2 \cdot \text{s}^{-1}$). However, when Shapiro et al. (2007) conducted cross-borehole hydraulic pump tests over 10s of metres, which included the presence of both high and low transmissivity fractures, the bulk rock-mass hydraulic conductivity was relatively low (10^{-7} $\text{m} \cdot \text{s}^{-1}$). This led Shapiro et al. (2007) to the important conclusion that the bulk rock-mass hydraulic connectivity is controlled by the less conductive intercon-

nected fractures, which act as hydraulic “bottlenecks” that impede groundwater flow. Furthermore, Shapiro et al. (2007) inferred that the discrete highly transmissive fracture zones were most likely not connected within the network. Their findings suggest a strong scale-dependency of the results collected from single wells (metres) versus results collected over multiple wells (10s of metres).

The key issues that are yet to be fully understood are how fracture network connectivity may change with increasing depth or be modified by secondary processes such as weathering, uplift and unloading and sub-surface fracture deformation. With a well-characterised fractured-rock aquifer, this study aims to: (1) describe the key elements that control hydraulic connection within a fractured rock aquifer; (2) provide examples where the effects of hydraulic connectivity can be recognised in both single well and catchment-scale hydrogeological datasets as well as surface and borehole electrical and electromagnetic geophysical surveys; and (3) demonstrate the role of in situ stress in modifying the inherent hydraulic connectivity of an aquifer through the use of stochastic, coupled hydromechanical (HM) models. This study is unique in that the field data is supported by representative large- and small-scale HM models, which demonstrate that changes in hydraulic connectivity are strongly influenced by fracture formation and deformation in response to the present-day in situ stress field. The inclusion of HM models is important as techniques such as outcrop mapping, borehole hydraulic and geophysical surveys do not account for sub-surface fracture deformation and its integrated HM response on a fracture network as a whole.

This study builds on an earlier study by Mortimer et al. (2011) which combined local- and regional-scale field hydrogeological datasets with stochastic HM models to investigate the influence of present-day in situ stress fields on groundwater flow patterns in shallow (<200 m depth) fractured-rock aquifers. A key conclusion of Mortimer et al. (2011) is that in situ stress does have a discernible effect at shallow depths in terms of variable fracture deformation distributions, which affect overall three-dimensional (3D) fracture network hydraulic conductivity, connectivity, anisotropy and groundwater flow rates. Whilst Mortimer et al. (2011) focussed on identifying and characterising the effects of in situ stress, this study differs by specifically focussing on the role of in situ stress in determining fracture network connectivity. This study uses the same datasets and models of Mortimer et al. (2011) plus additional surface and borehole geophysical datasets and more detailed small-scale HM models to better characterise and simulate features and processes that specifically affect fracture network connectivity.

Background

The key parameters that determine the overall connectivity of a fractured rock aquifer are the spatial distribution of fracture densities (fractures per unit volume), orientations (strike and dip), planar dimensions (area or trace extent)

and hydraulic apertures (NRC 1996). Of these, fracture density is considered one of the more critical parameters for connectivity with natural fracture networks tending to have fracture densities close to the percolation threshold (Renshaw 1996). Fracture density together with orientation and dimension determine the probability of multiple fracture intersections occurring within a rock mass volume. However, this information alone is insufficient as the distribution of fracture apertures and transmissivities of individual fractures and how they are linked within the network ultimately determine the overall permeability of a fractured rock medium (Long and Witherspoon 1985; Renshaw 2000). For example, the hydraulic conductivity of a fractured rock mass is extremely sensitive to its aperture as demonstrated by the “cubic law”. This law defines the hydraulic conductivity of an individual fracture idealized as an equivalent parallel plate opening. For an isolated test interval within a borehole, it is expressed as:

$$K_b = \frac{(2b)^3}{2B} \frac{\rho g}{12\mu} \quad (1)$$

where K_b is the bulk hydraulic conductivity ($\text{m}\cdot\text{s}^{-1}$) (where $K_b = \text{transmissivity}/\text{test interval}$), $2b$ is the fracture aperture width (m), $2B$ is the fracture spacing (m), ρ is the fluid density ($\text{kg}\cdot\text{m}^{-3}$), g is gravitational acceleration ($\text{m}\cdot\text{s}^{-2}$) and μ is the dynamic viscosity of the fluid (Pa.s).

The cubic law is a reasonable approach but unrealistic as it assumes that all fractures are infinite, planar, uniform and inelastic and that the bulk hydraulic conductivity of the medium is determined by the sum of contributions of all individual fractures (Snow 1969). In reality, the degree of fracture interconnection and fracture heterogeneity determines the bulk hydraulic conductivity of a fractured rock medium, which is often less than that predicted by the cubic law (Long and Witherspoon 1985).

With increasing depth comes increasing magnitudes of in situ stress, which results in progressive deformation of fracture apertures and progressive changes in fracture network hydraulics and connectivity. In general, stress fields are inhomogeneous and defined in simplified terms by three mutually orthogonal principal axes of stress, which are assumed to lie in the vertical (σ_v) and the maximum (σ_H) and minimum (σ_h) horizontal planes. In practice, far-field crustal stress regimes are classified using the Andersonian scheme, which relates the three major styles of faulting in the crust to the three major arrangements of the principal axes of stress (Anderson 1951). These stress regimes are: (1) normal faulting ($\sigma_v > \sigma_H > \sigma_h$); (2) strike-slip faulting ($\sigma_H > \sigma_v > \sigma_h$); and (3) reverse faulting ($\sigma_H > \sigma_h > \sigma_v$). Sub-surface fracture deformation in response to in situ stress has been shown to have a significant effect on fracture-network hydraulics and connectivity progressively with depth from the near surface (Barton et al. 1995; Mortimer et al. 2011). Stress-dependent fracture permeability manifests itself as fluid flow focussed along fractures which are favourably aligned within the in situ stress field and if fractures are critically stressed, this could impart significant permeability anisotropy to a fractured rock

mass. Specifically, preferential flow occurs along fractures that are oriented orthogonal to the minimum principal stress direction (due to low normal stress) or inclined $\sim 30^\circ$ to the maximum principal stress direction (due to dilation; Barton et al. 1995). The amount and rate of fracture deformation depends on several factors such as the nature of the contemporary stress field, depth, rock type, strata thickness, position within the overall stratigraphic sequence, relative mechanical contrasts between adjacent rock units and fracture “stiffness” (Price 1966; Van der Pluijm and Marshak 2004; Rutqvist and Stephansson 2003). Furthermore, fracture hydraulic apertures may be affected by processes such as mineralisation and detrital clay infill, which can partially or fully close fracture apertures hence altering the original transmissivity of individual fractures (Banks et al. 1996; Laubach et al. 2004).

The degree to which a fracture may deform is largely determined by its fracture stiffness, which is primarily a function of fracture wall contact area. Normal stiffness (jk_n) and shear stiffness (jk_s) of a fracture are measures of resistance to deformation perpendicular and parallel to fracture walls, respectively. Normal stiffness is a critical parameter that helps to define the hydraulic conductivity of a fracture via an estimate of the mechanical aperture as opposed to the theoretical smooth planar aperture as described in the cubic law. Estimates of fracture stiffness are derived by a variety of field logging or laboratory tests which are well documented in comprehensive reviews by Bandis (1993), Barton et al. (1985), Barton and Choubey (1977) and Hoek (2007). Standard practice is to derive stiffness estimates based upon fundamental measurements of fracture surface topography profiles and the elastic properties of the intact rock material. Ultimately, estimates of fracture stiffness attempt to account for more realistic fracture heterogeneity, asperity contact, deformation and tortuous fluid flow.

Methodology

The field site chosen for this investigation is the Wendouree Winery located within the Clare Valley, South Australia (Fig. 1). It is an ideal field site as it is underlain by a fractured-rock-aquifer terrain situated within a near horizontal, WNW–ESE directed regional compressional stress field that is seismically active and undergoing uplift and erosion (Sandiford 2003). The Wendouree field site is located approximately 2 km SSE of the township of Clare and it is a well-instrumented, multi-piezometer site located within the sub-vertical, overturned, western limb of the large “Hill River Syncline” structure. It contains several observation wells ranging in depths from 60–222 m which are all located within low porosity and permeability, thinly laminated (mm–cm), carbonaceous siltstones and dolomites of the Auburn Dolomite unit (Saddleworth Formation) over an area of $\sim 0.1 \text{ km}^2$ (Fig. 2; Love, 2003). Drill logs and core samples at Wendouree show that the weathered to

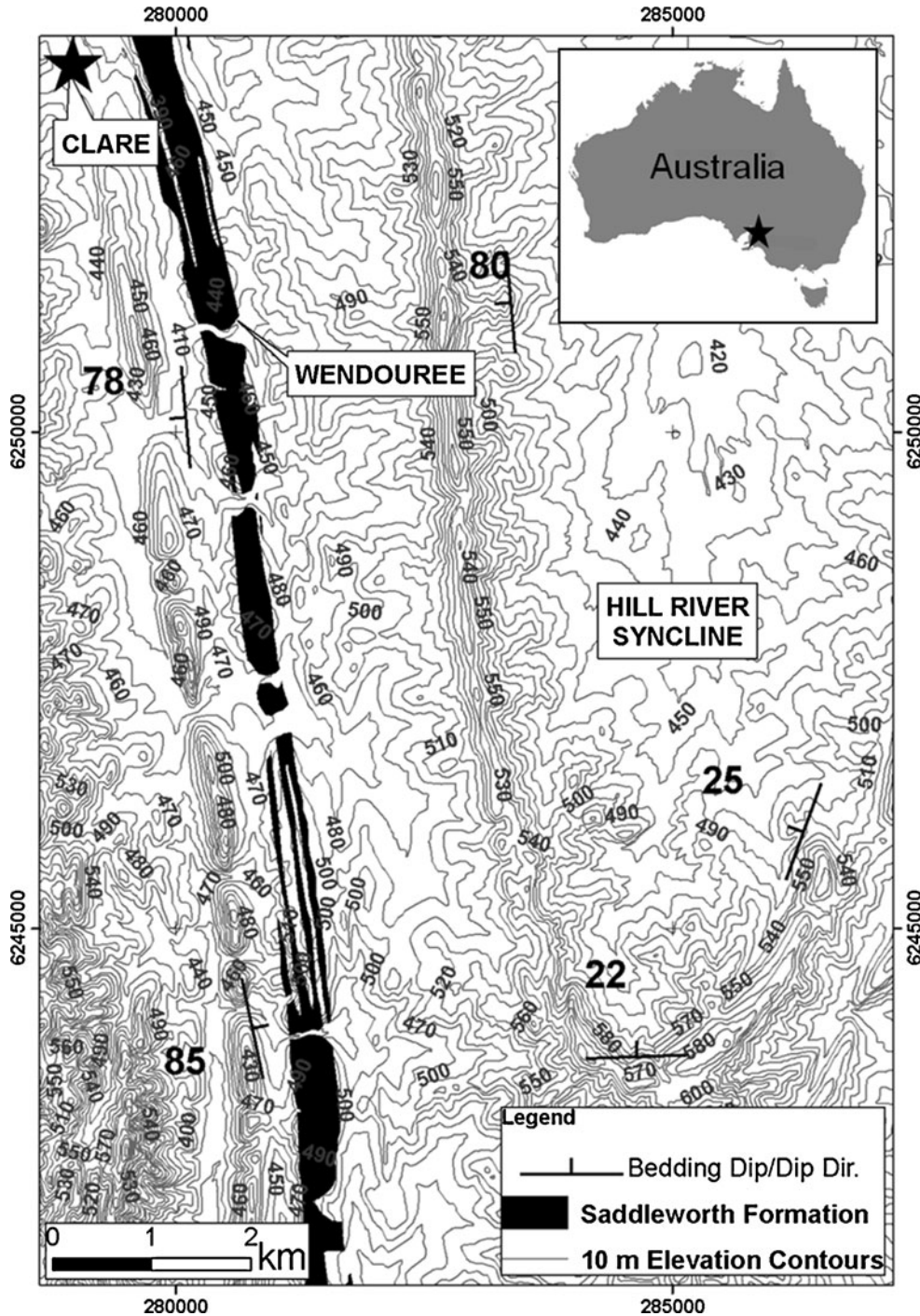


Fig. 1 Location of the Neoproterozoic (~730 Ma) *Saddleworth Formation* and *Wendouree* field site in the Clare Valley catchment with 10-m topographic contours. The basement geology is comprised of a layered sedimentary sequence that has been folded into the large *Hill River Syncline*. The *Wendouree* site is located on the overturned, western limb of this syncline (Geological Survey of South Australia 2001). Reprinted from Mortimer et al. (2011) with permission from Elsevier

fresh bedrock transition occurs at ~18 m depth below the surface.

The methodology of this study is the same as that of Mortimer et al. (2011) which involves the following three key steps:

1. A synthesis of the geological and hydrogeological setting from a review of the pre-existing data and knowledge of

the local- to regional-scale geology and hydrogeology. This includes fracture network characterisation results of Mortimer et al. (2011) which involved mapping of selected outcrops within the Hill River Syncline, limited drill core logging and in situ borehole fracture mapping and hydraulic characterisation at the *Wendouree* site. The in situ characterisation of the *Wendouree* fracture network was derived from the interpretation of coincident acoustic

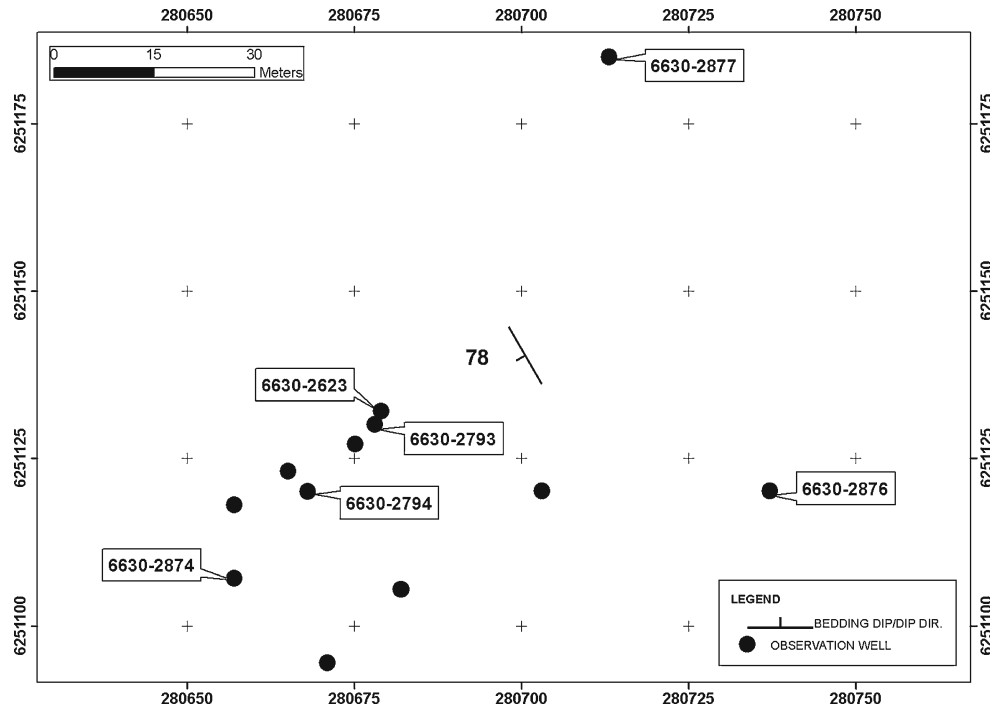


Fig. 2 The Wendouree multi-piezometer field site in the Clare Valley (PIRSA 2009). Reprinted from Mortimer et al. (2011) with permission from Elsevier

borehole televiewer (BHTV) and high-resolution temperature logs within four open wells (6630-2794, 6630-2874, 6630-2876 and 6630-2877) ranging from 90 to 222 m depth (Fig. 2). Similar to the methods of Barton et al. (1995) and Ge (1998), potentially hydraulically active fractures were identified based upon the coincidence of BHTV-imaged fractures with temperature gradient (dT/dx) anomalies indicative of advective groundwater flow in or out of a well. Other rock mass and fracture parameters were gained from limited-drill-core samples (well 6630-3068; Fig. 2) and scanline-fracture-mapping data of (T. Halihan, Flinders University, unpublished data, 1999). This study includes additional borehole electromagnetic (EM) flow meter (single inflatable packer) logs collected under pumped conditions for the same four observation wells.

2. Development of a conceptual Wendouree model based on the results of step 1.
3. Stochastic hydromechanical (HM) modelling of the conceptual Wendouree model using the two-dimensional (2D) Universal Distinct Element Code (UDEC). UDEC represents the rock mass as an assembly of discrete deformable, impermeable blocks separated by discontinuities (faults, joints, etc.) and can reproduce fully coupled HM behaviour (Itasca 2004). The basic HM model predicts the physical response of a fractured rock mass to an imposed stress field and the stress-displacement relationship of the medium, while satisfying the conservation of momentum and energy in its dynamic simulations with fluid-flow calculations derived from Darcy's Law (for a comprehensive review of the UDEC governing equations see Itasca 2004). In recent years, several researchers have successfully used UDEC to

investigate the link between rock deformation and fluid flow within fractured rock masses over a range of crustal depths, stress regimes, geological settings and fracture network geometries (e.g. Cappa et al. 2005; Gaffney et al. 2007; Min et al. 2004; Zhang and Sanderson 1996; Zhang et al. 1996).

In this study we use the same large-scale (100–200 m) cross-sectional and horizontal planar HM models of Mortimer et al. (2011). These models involve stochastic geometrical models based upon real but simplified data inputs and are not designed to produce a precise match to the field data but rather to demonstrate how sub-surface-fracture-deformation processes alter fracture network hydraulics and connectivity. In these models, rock-mass deformation was defined by the Mohr-Coulomb model and fracture behaviour was defined by the Coulomb-Slip criterion that assigns elastic stiffness, tensile strength, frictional, cohesive and dilational characteristics to a fracture (Itasca 2004). A comparison between deformed (stressed) and undeformed (zero stress) HM models is used as the basis for identifying the key features and processes that affect fracture network connectivity. Furthermore, this study includes the addition of small scale (1×1 m) HM models to demonstrate how variable sub-surface fracture deformation processes play a critical role in determining the bulk hydraulic conductivity of the fractured rock mass.

Geological setting

The Clare Valley catchment (~ 500 km²) is located approximately 100 km north of Adelaide, South Australia,

and lies within the northern Mount Lofty Ranges (Fig. 1). The Mount Lofty Ranges forms part of the “Adelaide Geosyncline”, which is a Neoproterozoic to Cambrian age (~827–500 Ma), thick (>10 km), rift-related sedimentary basin complex comprising of thinly laminated (mm) to thick (m) layered sedimentary strata (Preiss 2000). During the Middle–Late Cambrian “Delamerian Orogeny”, the rocks of the Clare Valley were subjected to low-grade greenschist facies metamorphism and three deformation events. This was a major episode of crustal shortening leading to strongly contractional, west-verging, thrust-faulting and NNW-trending folding (Preiss 2000). From the Delamerian Orogeny until the late Miocene period the Adelaide Geosyncline remained relatively tectonically stable (Preiss 1995). As southern Australia entered the late Miocene period (<10 Ma) a new phase of tectonic activity commenced, which was initiated by coupling and/or convergence between the Pacific and Australian plates (Hillis and Reynolds 2000; Sandiford et al. 2004). As a consequence, the Clare Valley is currently under near horizontal, approximately WNW–ESE-directed compression and related seismic activity, which correlates both spatially and temporally with ongoing fault activity along major range bounding faults of the Adelaide Geosyncline (Sandiford 2003). Evidence found on some of these major range-bounding faults suggest that the vertical component of their slip rates are in excess of tens of metres Ma^{-1} over the past 5 Ma leading to widespread uplift, erosion and the present-day topography of the Mount Lofty Ranges (Sandiford 2003).

There have been no in situ borehole stress-field data collected within the Clare Valley region; therefore, this study is based upon well-documented regional, far-field earthquake focal mechanism data, which are considered reliable and consistent indicators of far-field stress regimes and their orientation (Zoback 2007). In the year 2001, the town of Clare experienced nine small earthquakes up to magnitude 2.8, whilst in 1995, the nearby township of Burra recorded a significant magnitude 5.1 earthquake (PIRSA Minerals 1999; 2001). An evaluation of the focal mechanism for this particular Burra earthquake event revealed a reverse-faulting stress regime with near horizontal compression (σ_H) in a direction of 110° at a depth of 18–20 km with σ_h inferred to be mutually orthogonal at 020° . Although the region is undergoing horizontal compression at depth, the uppermost shallow crust is simultaneously experiencing widespread uplift, unloading and erosion (Sandiford 2003). That is, the uplift and unloading processes affecting the Mount Lofty Ranges are concurrent with and in direct response to the far field tectonic compression. It is not known to what depth the effects of uplift and unloading occur in this region but studies elsewhere in the world have shown that it could extend a few hundreds of metres to 1 km below the surface (Engelder 1985; Hancock and Engelder 1989). The focus of this study is on the upper 200 m depth horizon, which is inferred to be under the influence of a normal stress regime that involves isotropic, lateral relaxation of the rock mass consistent with the effects of

uplift and unloading (i.e. $\sigma_v > \sigma_H = \sigma_h$). This inference is appropriate given that relaxation of the rock mass is expected to be near complete, considering that the total regional uplift has been estimated at greater than 200 m and that erosion processes are known to be occurring at a rate faster than that of uplift (Sandiford 2003).

Outcrop mapping exercises conducted at several locations across the Clare Valley found a consistent joint set pattern present within the various layered rock units of the Hill River Syncline. In addition to bedding planes, there are four joint set structures including sub-vertical “ac” (extension) joints, sub-horizontal “bc” (extension) joints and two moderately dipping conjugate “hk0” (shear) joints, which together produced a pattern typical of jointing in response to simple folding of a layered sedimentary sequence (Price 1966; Van der Pluijm and Marshak 2004) during the Delamerian Orogeny (Fig. 3). Only the joint density varied at each outcrop as determined by each rock type, thickness and position within the sequence, i.e. a stratabound joint formation pattern. It is this palaeo-stress regime and its associated deformation, which is the primary control on the development of fracture networks and fracture permeability within the fractured rock aquifers of the Clare Valley.

Hydrogeological setting

Within the Clare Valley catchment there are relatively consistent and distinctive groundwater patterns. For example, Fig. 4 is a plot of measured well yield (normalised against the total well depth, $\text{L.s}^{-1}.\text{m}^{-1}$) for

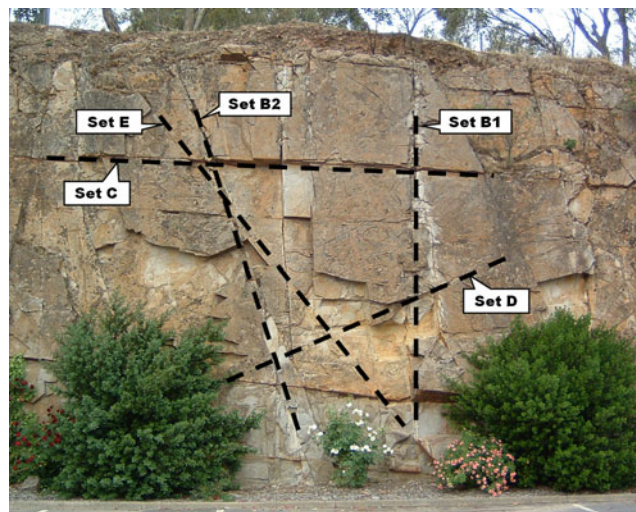


Fig. 3 ENE-looking, longitudinal section view of a near vertical bedding plane within the Saddleworth Formation (Auburn Dolomite unit) located on the western limb of the Hill River Syncline (~5 m high rock face). This outcrop exposure contains the same rock unit and structures as that intersected in drill holes at the Wendouree site located ~2 km to the SSE. Note the five fracture sets typical of this area: bedding planes (set A); “ac” (extension) joints (sets B1 and B2); sub-horizontal “bc” (extension) joints (set C) and conjugate “hk0” (shear) joints (sets D and E). Reprinted from Mortimer et al. (2011) with permission from Elsevier

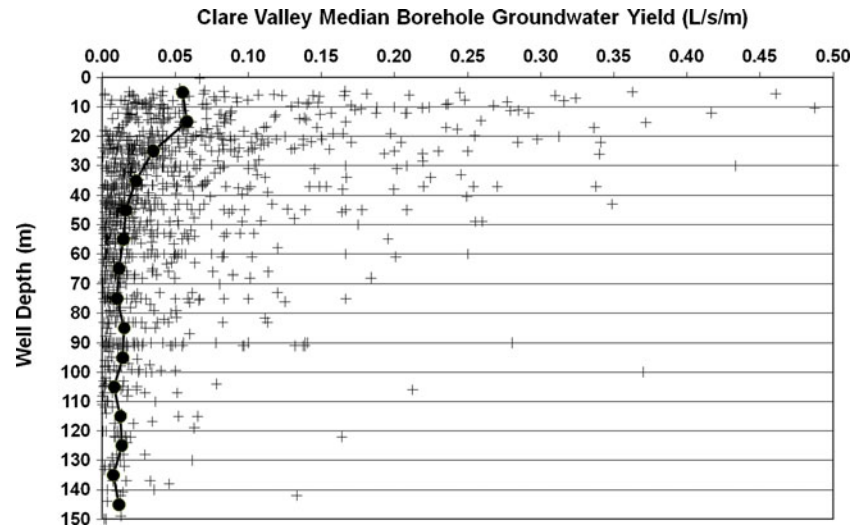


Fig. 4 Clare Valley catchment-wide groundwater well yields whereby each well-yield value was normalised against the total depth of the well then plotted against the total depth of the well ($\text{L}\cdot\text{s}^{-1}\cdot\text{m}^{-1}$, $n=1,316$ drill holes). The + symbols represent individual data points, whilst the *connected solid circles* represent the calculated median yield per metre for 10-m-thick depth intervals below the surface (PIRSA 2009). Note that the weathered-to-fresh rock transition across the catchment generally occurs at <20 m depth below the surface. Reprinted from Mortimer et al. (2011) with permission from Elsevier

all wells recorded within the catchment versus the total depth of the well. The large majority of these wells are open and used for domestic/agricultural purposes. Compared to near surface (0–10 m depth), median groundwater yields have decreased ~ 3 and ~ 4 fold at approximately 40 and 100 m depth below the surface, respectively, suggesting the existence of a hydraulic discontinuity at ~ 40 m depth below the surface (Fig. 4). This regional well-yield dataset is independent of lithology and position within the overall folded sequence, nor can this vertical trend be explained by near-surface weathering. A review of a significant volume (hundreds) of geological water well logs sourced from the State Government online database show that, across the catchment, the depth of weathering is typically <20 m below the surface (PIRSA 2009). This regional, vertical, groundwater yield trend was also observed on a local scale at the Wendouree site as demonstrated by electromagnetic (EM) flow-meter profiles collected as part of this study (Fig. 5). These EM flow-meter profiles reveal the flow distribution entering the well and also show a very sharp decrease to almost negligible groundwater flow rates commencing from approximately 40–60 m depth below the surface (Fig. 5). Again, this local vertical groundwater flow trend cannot be explained by the near-surface weathering profile (~ 18 m depth) or by any variance in the uniform carbonaceous silt and dolomite host rocks. These regional- to local-scale field observations suggest that vertical groundwater flow profiles are influenced by some other regional-scale factor controlling depth-dependent changes in fracture hydraulic connectivity.

Evidence cited by Love (2003) from piezometer pumping tests and ^{222}Rn -concentration depth profiles at Wendouree revealed that the hydrogeology is characterised by high spatial variances in bulk hydraulic conductivity (K_b) values and groundwater flow rates in the upper

100 m depth horizon (Fig. 6). ^{222}Rn is produced from in situ decay of ^{238}U within the aquifer and because of its short half-life (3.83 days) it is used to locate zones of active groundwater flow into wells and as a proxy for lateral flow rates (Love et al. 2007). That is, relatively high ^{222}Rn concentrations in groundwater indicates high flow rates within fractures that rapidly transport ^{222}Rn to the well prior to it decaying below detection limits. Together, these Wendouree K_b and ^{222}Rn profiles provide an indication of transmissivities and groundwater flow rates as a function of depth and also suggest the presence of a significant hydraulic discontinuity located at ~ 40 m depth below the surface that is not coincident with the known weathered-to-fresh rock transition located at ~ 18 m depth. The pumping test and ^{222}Rn data are supported by ^{14}C , CFC-12 and ^3H data collected from the same piezometers. These environmental tracers all show modern groundwater ages within the upper 40 m depth horizon, indicating rapid vertical circulation, whilst more ancient groundwater occurs at >40 m depth (Love 2003). Estimates of vertical recharge rates at Wendouree from the ^{14}C groundwater age profiles were $\sim 20 \text{ mm}\cdot\text{year}^{-1}$ for the upper system (<40 m depth) and $<0.2 \text{ mm}\cdot\text{year}^{-1}$ for the lower one (>40 m depth; Love 2003). This suggests that there is minimal hydraulic connection and vertical leakage between these two horizons, a phenomenon also observed elsewhere in the catchment (Cook et al. 2005). Regardless of depth, anomalous spikes in ^{222}Rn and ^{14}C concentrations were also found to coincide with major electrical conductivity, temperature and pH discontinuities, indicating the presence of significant hydraulically active fractures and advective groundwater flow at specific down-hole locations (Love 2003). However, it is clear from the data presented in Figs. 4, 5 and 6 that, at shallow depths (<40 m), the system is hydraulically more active than at greater depths (>40 m).

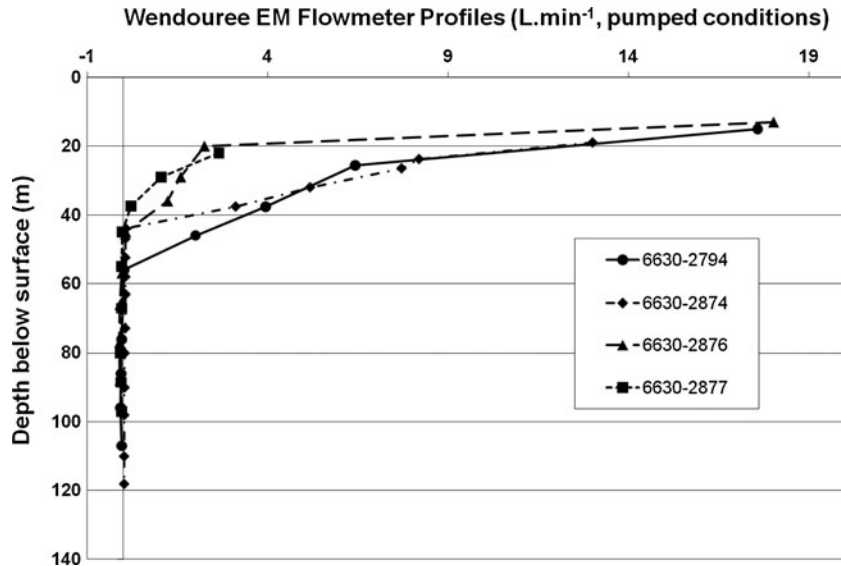


Fig. 5 EM flow-meter profiles under pumped conditions ($20 \text{ L}\cdot\text{min}^{-1}$) for four Wendouree observation wells (wells 6630-2794, 6630-2874, 6630-2876 and 6630-2877; see Fig. 2) located over an area of $\sim 100 \text{ m}^2$

In an attempt to detect hydraulic connection between boreholes at Wendouree, Love et al. (2002) conducted a pump-packer test and observed water-level changes in a piezometer nest located approximately 14 m to the NE of the pumped borehole (well 6630-2794; Fig. 2). This test suggested that a strong vertical connection existed between piezometers located in the upper 0–40 m depth horizon and the packer interval located between 60–65 m depth. At piezometer depths of between 40–75 m, the packer test recorded variable but lower degrees of hydraulic connection, whilst at depths $>80 \text{ m}$, the two deepest piezometers recorded no hydraulic connection. This pump-packer test

data further supports the existence of decreasing levels of hydraulic connectivity with increasing depth and the presence of a significant hydraulic discontinuity located at approximately 40 m depth below the surface.

At Wendouree, Mortimer et al. (2011) analysed coincident acoustic BHTV and high-resolution temperature logs from four open wells (6630-2794, 6630-2874, 6630-2876 and 6630-2877) ranging from 90 to 222 m depth (see Fig. 2). The stereographic analysis of the 626 fractures imaged with the BHTV revealed five distinct fracture sets that correlate with bedding and joint-set measurements recorded from nearby outcrop and elsewhere within the Clare Valley, i.e. the five geological structures typical of the region (sets A–E; see Fig. 3). Furthermore, an evaluation of the population distribution and orientations of the interpreted hydraulically active fractures indicated that steeply dipping ($>70^\circ$) bedding planes and joints are dominantly the most hydraulically active fractures (Mortimer et al. 2011). They represented the approximately orthogonal NW–SE striking bedding plane (set A) and the NE–SW striking “ac” joint set (set B). This interpretation is plausible given the uplift and unloading stress regime expected at these shallow depths, which should favour steep-dipping structures under conditions of isotropic, lateral relaxation of the rock mass.

In a different Clare Valley study, Skinner and Heinson (2004) conducted several electromagnetic (EM) surface and direct current (DC) surface, borehole-to-surface and borehole-to-borehole geophysical surveys at several sites across the catchment including Wendouree. The purpose of their study was to attempt to use electrical and electromagnetic techniques to detect hydraulic pathways within heterogeneous fractured-rock aquifers based on the theory that saline-fluid-saturated fractures are relatively more electrically conductive than their impermeable host rock matrix and can distort the local potential field (Skinner and Heinson 2004).

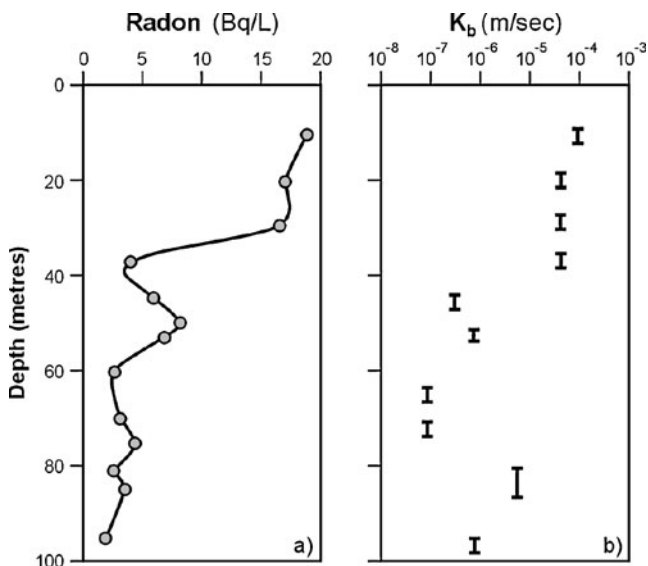


Fig. 6 An example of ^{222}Rn and bulk hydraulic conductivity (K_b) profiles at Wendouree: **a** ^{222}Rn ($\text{Bq}\cdot\text{L}^{-1}$) open well profile (well 6630-2623); and **b** K_b ($\text{m}\cdot\text{s}^{-1}$) estimates from piezometer pump test (wells 6630-2623 and 6630-2793). The vertical bars of the K_b profile represent the length of the slotted piezometer interval (Love 2003)

Specifically at Wendouree, Skinner and Heinson (2004) conducted a surface EM azimuthal survey with EM34 coplanar transmitter-receiver coils in both horizontal and vertical coil orientations (well 6630-2874; Fig. 2). This method involved rotating these coils around a selected borehole whilst recording variations in the resistivity of the ground as a function of geographical orientation (azimuth). Figure 7 shows a comparison of the results of two surface EM azimuthal resistivity surveys completed at 10 and 40 m dipole separation distances. The results are depicted as contoured polar plots of calculated apparent electrical conductivity versus azimuth with the calculated apparent conductivity being the weighted average over the penetration depth of the signals, where the weighting depends on the coil orientation and separation. These results reveal that at 10 m dipole separations the direction of maximum apparent electrical conductivity is near symmetrical yet subtly elongated in a NNW–SSE direction. At 40 m dipole separations, this elongation becomes more pronounced with the increased anisotropy being attributed to greater depth penetration and spatial resolution of steeply dipping, conductive fractures, particularly with the vertical-coil configuration. A similar asymmetrical-shaped geophysical anomaly was recorded at Wendouree with a DC borehole-to-surface survey, which found the highest electrical potential was oriented NNW–SSE with a down-dip direction to the WSW coincident with the strike and dip of the bedding planes (Skinner and Heinson 2004). These methods can be considered analogous to determining the maximum permeability direction of a fractured rock aquifer, which in this case, is aligned with the strike of the bedding planes at the site. This finding was repeated at several other locations throughout the Clare Valley, which suggests that bedding planes are the dominant hydraulically active fractures within the catchment (Skinner and Heinson 2004).

These surface and borehole-to-surface geophysical surveys were used to define the dominant hydraulically conductive fractures at each site. However, to test the

hydraulic connectivity between boreholes requires the use of DC cross-borehole surveys. In this method, a known current is individually driven through electrodes at specific down hole positions in one borehole, whilst simultaneously measuring the potential voltage at the same intervals down a second borehole as referenced against a zero potential electrode at the surface. At Wendouree and elsewhere within the catchment, these cross-borehole surveys found several extensive, shallow dipping to horizontal conductive structures at depths ranging from ~20–60 m below the surface (Skinner and Heinson 2004). At another Clare Valley site, located ~12 km south of Wendouree, 2.5D inverse modelling of DC cross-borehole data revealed an approximately horizontal fracture of low resistivity extending across the ~60 × 30 m survey area and, although it was discernible in all orientations, its anomalous signature was more enhanced where it intersected steep-dipping bedding planes (Skinner and Heinson 2004). This conclusion is significant as it highlights that both the electrical and electromagnetic surface and borehole surveys not only found groundwater flow within the catchment being dominated by flow along steep-dipping bedding planes but that it also involves lateral flow being facilitated by low-angle intersecting fractures. Like the other datasets and conclusions presented in this study, the results of these geophysical studies were consistent across several sites regardless of lithology and position within the Hill River Syncline and helped to define the two distinct upper and lower groundwater flow systems in the Clare Valley (Skinner and Heinson 2004).

Conceptual model

Mortimer et al. (2011) combined all of the above data and field observations to develop the conceptual Wendouree fracture network model consisting of a densely fractured, clay-rich, weathered, upper zone (0–20 m), a less fractured

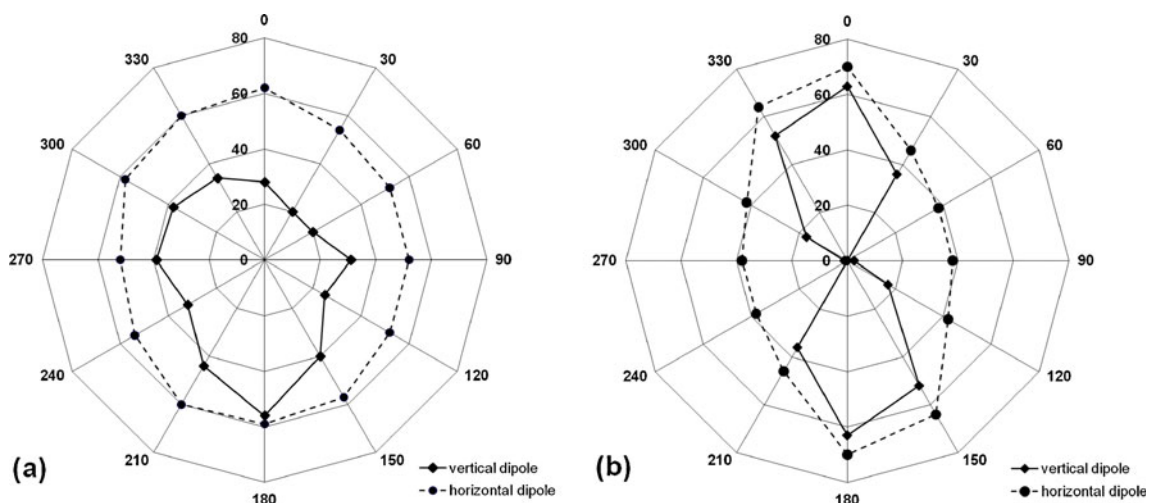


Fig. 7 Polar plots of surface EM resistivity azimuthal data collected at well 6630-2874 **a** 10 m and **b** 40 m dipole separations (units of Ωm) for both vertical (*diamonds*) and horizontal (*circles*) dipole orientations

transitional zone (20–40 m) and a low fracture density zone (>40 m; Fig. 8). With increasing depth there is a trend of decreasing fracture density based upon a reduction in the number of finite joint sets (sets B, C, D and E) against a persistent background of high-density bedding planes (set A). This trend has been observed within the limited amount of diamond drill core samples available plus the BHTV logs. The primary cause of this fracture density trend is attributed to the effects of uplift and unloading. For example, the Wendouree BHTV logs revealed a proportionally greater amount of sub-horizontal joints in the upper 40 m depth horizon, which is considered indicative of neotectonic joint formation in response to unloading (Hancock and Engelder 1989). Thus, the increased development of unloading-related, sub-vertical flexural and sub-horizontal sheeting (or relaxation) joints closer to the surface creates a distinct zoning of the vertical fracture density profile throughout the entire aquifer system. In addition, as depth increases so too will the magnitudes of stress resulting in the progressive deformation of fracture apertures. With increasing depth and stress magnitudes progressive fracture aperture deformation will lead to progressive changes in fracture network hydraulics and connectivity. Overall, the most significant hydraulically conductive fractures are expected to be the steeply dipping fractures (sets A and B), considering that the vertical stress is the major principal stress.

Fracture network connectivity models

The philosophy of this HM modelling exercise is to demonstrate the process of fracture deformation and its

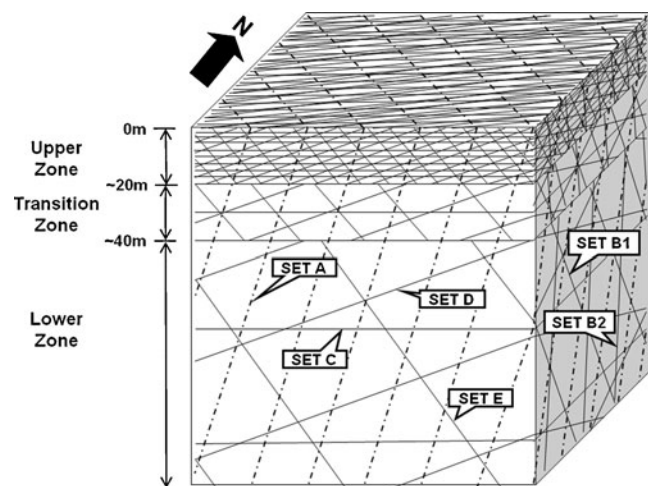


Fig. 8 Schematic diagram of the Wendouree conceptual fracture network model showing decreasing joint densities between the upper, transition and lower zones. *Dashed lines* denote the persistent, dense, bedding planes of *set A*, whilst the *solid lines* represent joint sets *B*, *C*, *D* and *E*. The NE–SW cross-sections and horizontal planar models of section [Groundwater flow models](#) are oriented in the plane of sets *B* and *C*, respectively. Reprinted from Mortimer et al. (2011) with permission from Elsevier

influence on network hydraulic connectivity with representative 2D fracture network models under shallow depth conditions. These models are constrained and correlated with known geology and groundwater flow observations; however, these models are not designed to produce a precise match to the field data but to help demonstrate how the process of sub-surface fracture deformation alters fracture network connectivity and fluid flow. This includes the use of stochastic geometrical models based upon real but simplified data inputs that can identify groundwater flow trends and the key features and processes that have the most influence across small to large scales. To identify the key processes that determine fracture network hydraulics and connectivity necessitates the use of HM models at two different scales. Specifically, this study utilised the large-scale (100–200 m block size) stochastic models of Mortimer et al. (2011) to demonstrate the effects of depth-dependent changes in fracture density and sub-surface fracture deformation processes on groundwater flow. The addition in this study of small-scale (1 × 1 m block size) models is designed to help visualise how the inherent fracture network connectivity can be altered by secondary processes such as sub-surface fracture deformation as well as to test both quantitatively and qualitatively the observations of Shapiro et al. (2007).

Model design

The large-scale stochastic, 2D Wendouree UDEC models are based upon the conceptual fracture-network model (see Fig. 8) and are simple 100–200 m size, cross-section and planar models built from the surface down (Fig. 9a and b). The small-scale 1 × 1 m model is a horizontal planar model that represents a sample snapshot of the larger-scale models at a depth of 100 m below the surface (Fig. 9c). These 2D models describe a geometrical reconstruction that consist of 2D vertical or horizontal planar slices of the conceptual fracture network model which incorporate the effects of the 3D stress field (i.e. σ_v , σ_H , and σ_h). The blocks defined by the fracture network generated within UDEC were discretized into a triangular mesh of constant strain with the nodal distances varying from 1.5 m (large-scale models) to 0.15 m (small-scale models).

As this study is focussed on the upper 200 m depth horizon, a normal stress regime is employed with the HM models to simulate isotropic, lateral relaxation of the rock mass consistent with the effects of uplift and unloading (i.e. $\sigma_v > \sigma_H = \sigma_h$). The magnitudes of stress within these models are based upon an estimate of σ_v (i.e. $\rho \cdot g \cdot h$) and applied as a differential stress ratio compatible with the prevailing normal stress regime (i.e. $\sigma_v > \sigma_H = \sigma_h$ at a ratio of 1: 0.5: 0.5). The 2D planar and cross-section models enabled σ_H to be perpendicular to the model boundaries, i.e. σ_H at 110°. The cross-section orientation is approximately parallel to the E–W hydraulic gradient recorded at the Wendouree site (Love 2003) and used apparent dips for oblique fracture sets.

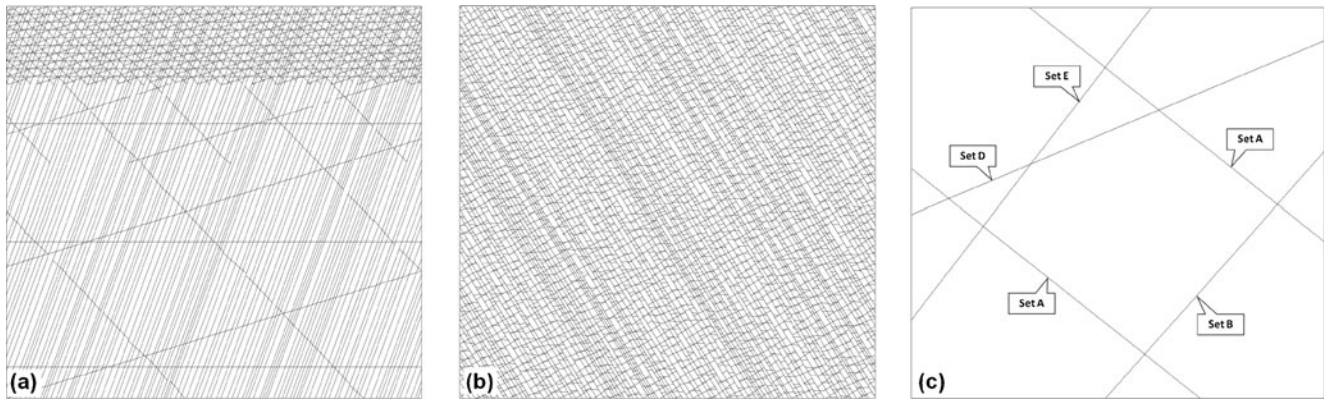


Fig. 9 Example stochastic 2D Wendouree UDEC models: **a** the 100×100 m NE–SW vertical-cross-section model, in the plane of set B, which is dominated by the dense bedding planes of set A; **b** the 100×100 m horizontal planar model, in the plane of set C, at 20 m depth below the surface; and **c** 1×1 m horizontal planar model with finite difference mesh in the plane of set C at 100 m depth below the surface. Figure 9a and b reprinted from Mortimer et al. (2011) with permission from Elsevier

The principal-stress orientations are assumed to be the same as that determined for the far-field (deep) reverse-faulting stress regime, which is a reasonable assumption as studies on shallow, neotectonic joint formation within sedimentary sequences found unloading and release joints related to uplift and erosion strike approximately parallel and perpendicular to the regional maximum horizontal stress direction (Engelder 1985; Hancock and Engelder 1989). The fracture network was based on the conceptual model (Fig. 8), whilst other fracture parameters were derived from nearby scanline fracture mapping data (Table 1; T. Halihan, Flinders University, unpublished data, 1999). The bedding plane to joint set density ratio consists of 2:1 in the upper zone, 16:1 in the transitional zone and 32:1 in the lower zone (see Fig. 9a). These joint set densities are estimates only, as the precise values are unknown due to the limited and biased nature of both the vertical drill core samples and BHTV logs. However, these joint set densities are reasonably comparable to those determined from the BHTV logs and this model design resulted in a reasonable correlation with the known groundwater flow observations (see section Discussion).

Fluid pore pressures were based on an assumed hydrostatic gradient with fluid flow allowed to occur in any direction within the fracture network under the imposed hydraulic gradient. Rock mass and fracture parameters were derived from geotechnical logging and ultrasonic velocity testing of limited drill core samples, Mohr circle analysis and other empirical relationships that

are compatible with published values (Table 2; Kulhawy and Goodman 1980; Nordlund et al. 1995; Waltham 2002). A comprehensive description of the model conditions and parameters used in this study is provided in Mortimer et al. (2011).

Of critical importance to this study is the highly variable joint stiffness distributions recorded for each individual fracture set (Mortimer et al. 2011). Therefore, the ranges of normal (jk_n) and shear (jk_s) stiffness values were taken as normally distributed across all fractures within the model (Table 2). Specifically, each individual fracture within the model may consist of up to several separate segments, 0.15 m (small-scale models) to 1.5 m (large-scale models), with randomly assigned jk_n and jk_s values. The objective of this approach is to better account for naturally occurring fracture heterogeneity such as asperity and contact area distribution, mineralization, etc., and ultimately heterogeneity in deformation and fluid flow along individual fracture planes. Fracture friction and dilation angles were both inferred as zero as these parameters largely dictate the mode of fracture deformation rather than the relative deformation trends occurring across the different fracture sets within the fracture network, which was the main focus of this study. At Wendouree, the mean fracture aperture measured from nearby outcrop was ~100–200 μm and ranged up to a maximum of 1.2 mm (Love et al. 2002); however, for the purposes of this modelling exercise, a reference aperture value of 0.5 mm is considered appropriate to facilitate the

Table 1 Mean fracture orientation (standard deviation, SD), classification, trace (SD), and spacing for the upper, transition and lower zones of the Wendouree stochastic UDEC models. Note that the set A fractures are designed to transect the entire model with a fixed orientation in order to represent planar, continuous bedding plane surfaces and that the NE–SW cross-section models use modified apparent dips

Fracture set	Mean dip & Dip direction	Classification	Mean trace (m)	Mean spacing (m)
A	78(0) / 240(0)	Bedding planes (“S ₀ ”).	>100	0.5–1.5
B1	78(9) / 331(10)	Steep-vertical, “ac” (extension) joints.	6 (5)	2, 16, 32
B2	75(6) / 155(9)	Steep-vertical, “ac” (extension) joints.	6 (5)	2, 16, 32
C	2(6) / 013(33)	Sub-horizontal, “bc” (extension) joints.	11 (18)	2, 16, 32
D	38(4) / 356(13)	D & E - conjugate pair of “hk0” (shear) joints.	2 (1)	2, 16, 32
E	54(5) / 146(9)	D & E - conjugate pair of “hk0” (shear) joints.	6 (5)	2, 16, 32

Table 2 Rock mass and fracture parameters used to construct the Wendouree UDEC HM models. Source: 1 core sample ultrasonic velocity tests; 2 Mohr circle analysis; 3 core sample derived fracture JRC profiles and elastic moduli relationships; 4 inferred; and 5 approximate values for fresh water at 20°C. Reprinted from Mortimer et al. (2011) with permission from Elsevier

UDEC model parameters	Value	Units	Source
Rock material density (ρ)	2732	kg.m ⁻³	1
Poisson's ratio (ν)	0.27	-	1
Young's modulus (E)	77e6	Pa	1
Bulk modulus (K)	96e9	Pa	1
Shear modulus (G)	30e9	Pa	1
Cohesion (c)	19e6	Pa	2
Friction angle (ϕ)	54	Degrees	2
Dilation angle (ψ)	0	Degrees	4
Uniaxial compressive strength	128e6	Pa	2
Tensile strength	8.5e6	Pa	2
Joint normal stiffness (jk_n)	7.7–35.1e9	Pa.m ⁻¹	3
Joint shear stiffness (jk_s)	3.0–13.6e9	Pa.m ⁻¹	3
Joint cohesion	0	Pa	4
Joint tensile strength	0	Pa	4
Joint friction angle	0	Degrees	4
Joint dilation	0	Degrees	4
Joint aperture (at zero stress)	0.5	mm	4
Joint residual aperture	0.1	mm	4
Joint permeability constant (1/12 μ)	83.3	(Pa.s) ⁻¹	5
Water density	1000	kg.m ⁻³	5

observation of overall fracture network deformation patterns. The choice of this initial aperture value is not considered critical, as the main objective is to explore the relative effects of the in situ stress field on individual fracture sets.

Fracture deformation model

To assess the effect of fracture geometry within the applied normal stress regime, the amount of fracture deformation across all individual fracture sets as a function of depth was analysed for a 200 × 200 m Wendouree NE–SW vertical cross-section (see Figs. 8 and 9a). The deformation patterns of individual fracture sets provide a basis to evaluate the ultimate HM response of a fractured rock mass to the applied stress. UDEC calculates the effective hydraulic aperture of a fracture based upon its initial fracture aperture width at zero stress plus any normal displacement (positive or negative) that has occurred as a result of deformation. This fracture deformation data is depicted for each individual fracture set in terms of the amount of fracture closure normal to fracture walls, commencing with an initial hydraulic aperture of 0.5 mm at the surface (Fig. 10). The fracture deformation profiles of Fig. 10 show a divergence in the relative amounts of fracture deformation occurring across the individual fracture sets commencing from approximately 50 m depth. In particular, the rate of fracture closure with depth is approximately uniform for the moderate dipping to sub-horizontal joint sets (sets C, D and E), whilst the steep-dipping bedding planes (set A) close at a lesser rate. Using these closure estimates, the reduction in equivalent parallel-plate hydraulic conductivities for individual frac-

tures can be derived from the cubic law (Eq. 1). For example, at a depth of 185 m, the average fracture hydraulic conductivities for the steep-dipping bedding planes (set A) and the moderate dipping to sub-horizontal joint sets (sets C, D and E) are reduced by ~54 and ~62–71%, respectively. This progressive development with depth of an anisotropic permeability orientation along steep-dipping fractures highlights the important role of fracture geometry in regards to stress-dependent fracture permeability. This result is attributed to the fact that the applied normal stress field simulates uplift and unloading through isotropic, lateral relaxation across the entire rock mass, which should result in less deformation occurring along steep-dipping fractures. Note, lastly, that the local departures from the general trends are attributable to random assignment of the fracture stiffness values.

Groundwater flow models

Vertical cross-section flow model

To investigate overall fracture network hydraulics and connectivity, an analysis of groundwater flow through both the deformed (stressed state) and undeformed (zero stress state) Wendouree NE–SW cross-sectional models was completed. For the deformed model, this process involved deforming the model under normal stress regime conditions before subjecting it to steady state, groundwater flow under an E–W oriented hydraulic head gradient of 0.01 and 0.001, which fits with the measured seasonal Wendouree hydraulic gradient of between 0.003 and 0.007 (Love 2003). Like the fracture deformation models, the initial fracture hydraulic aperture for the groundwater flow models was set at 0.5 mm. The process for the undeformed model is identical except that fracture hydraulic apertures are fixed for all depths at 0.5 mm. UDEC assigns equivalent hydraulic conductivities to each uniform aperture (parallel plate) segment of a fracture according to the cubic law (Eq. 1). The flow rate through each of these segments is calculated using Darcy's Law:

$$q = \frac{(2b)^3}{12\mu} \frac{\Delta P}{L} \quad (2)$$

where q is the fracture flow rate per unit width normal to flow direction (m².s⁻¹), ΔP is the pressure difference (Pa), L is the length of each segment (m).

Vertical depth profiles of UDEC derived fracture flow rates (m².s⁻¹) and field data such as the normalised borehole yields (L.s⁻¹.m⁻¹; see Fig. 4) are not directly comparable; therefore, a comparative analysis of these UDEC results can only be qualitative. The results of the UDEC vertical cross-section flow models are depicted in terms of mean apertures and flow rates for all fractures within 10 m thick horizontal depth intervals with the weathered zone represented by the upper 20 m of the model (Fig. 11a and b). Figure 11a shows a uniform, linear decrease in mean apertures with depth, whilst the decrease

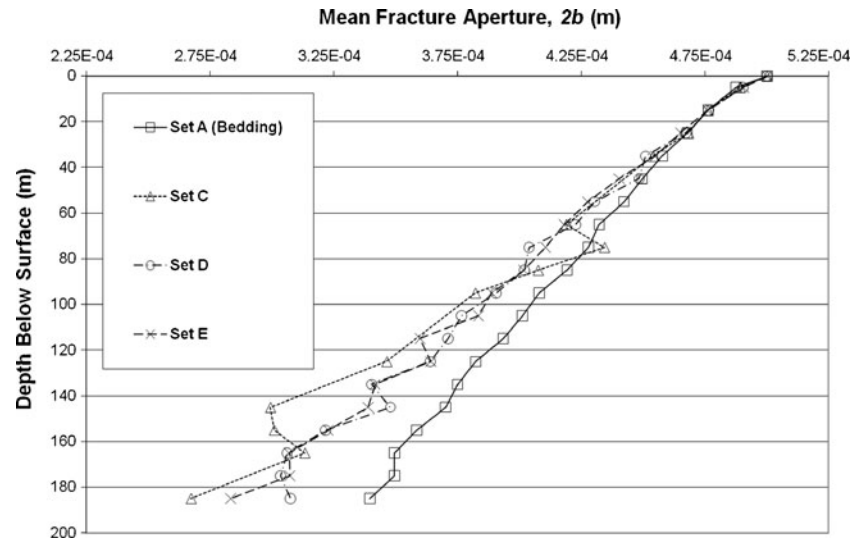


Fig. 10 UDEC fracture deformation depth profiles of the individual fracture sets that comprise the Wendouree NE-SW cross-sectional model under a normal stress regime. The initial fracture hydraulic apertures were set at 0.5 mm with data points representing the calculated mean fracture aperture for each 10 m thick depth interval. Reprinted from Mortimer et al. (2011) with permission from Elsevier

in mean flow rates is non-linear and resembles the regional well groundwater yield trend of Fig. 4. When the deformed Wendouree fracture network flow model is compared against an undeformed version of the same model (Fig. 11b), the applied normal stress regime appears to have had an effect, as the trend of decreasing mean fracture flow rates with depth in the undeformed state is distinctly different and only minimal. As both of these models use an identical fracture network configuration, this difference is attributed to stress-related, fracture deformation processes that progressively modify fracture apertures and permeability. Furthermore, this progressive fracture deformation also leads to changes in hydraulic connectivity and flow patterns within the overall fracture network. Although this is difficult to ascertain from this data, particularly as the 2D cross-section model becomes dominated by the relatively higher conductivity, steeply dipping bedding planes with increasing depth.

Hydraulic conductivity ellipses

The potential influence that the imposed stress field may have on the permeability tensor of the Wendouree fracture network model was evaluated by comparing deformed and undeformed models through the estimation of 2D planar hydraulic conductivity ellipses. This process involved slicing the conceptual Wendouree fracture network model into horizontal, planar depth slices at 20, 40, 75 and 100 m depths (see Figs. 8 and 9b). These four depth slices were chosen to capture both the increasing effects of stress and decreasing joint densities that occur with depth. Like the vertical cross-section flow models, these planar models use a normal stress regime to simulate the effects of uplift and unloading. Similar to the methodologies of Min et al. (2004) and Zhang et al. (1996), each planar model was deformed under their corresponding depth-dependent magnitudes of stress. These deformed models were then subjected to

steady-state, fluid flow under an applied E-W hydraulic gradient of 0.01, with the north and south boundaries acting as impermeable no-flow barriers. The effective hydraulic conductivity (K) of each model is estimated using Darcy's Law below and the UDEC sum of discharge flow rates (Q) from each steady-state model:

$$Q = KAi \quad (3)$$

where Q is the sum of discharge flow rates ($\text{m}^3 \cdot \text{s}^{-1}$), K is the effective hydraulic conductivity ($\text{m} \cdot \text{s}^{-1}$), A is the cross-sectional area normal to the flow direction (m^2) and i is the hydraulic gradient.

To estimate the 2D hydraulic conductivity ellipse at a particular depth slice, the value of K is calculated for the initial fracture network model using the method described in the previous, then this entire process is repeated for $6 \times 30^\circ$ (i.e. 180°) horizontal rotations of the identical model. The 2D hydraulic conductivity ellipse is then constructed by plotting the value of K recorded at each 30° horizontal model rotation. For comparison, this exercise is repeated for the same fracture network models but under a zero stress field, i.e. the undeformed state with fixed apertures. The initial (and zero stress) fracture aperture was set at 0.5 mm.

The model results show that at each depth slice the hydraulic conductivity ellipses are all elongated in a WNW-ESE direction (i.e. a strike direction of $300-120^\circ$; Fig. 12a-d). This elongation direction represents the maximum K direction and is close to the strike of the extensive, densely spaced bedding planes (set A, $330-150^\circ$). The NNE-SSW direction of the minimum K direction approximates, but is slightly offset to, the strike of the less dense, finite length joint sets (sets B, D and E). The orientation and shape of these K ellipses are in agreement with those estimated from the surface EM azimuthal resistivity surveys of Skinner and Heinson (2004; see Fig. 7). This near coincidence of the

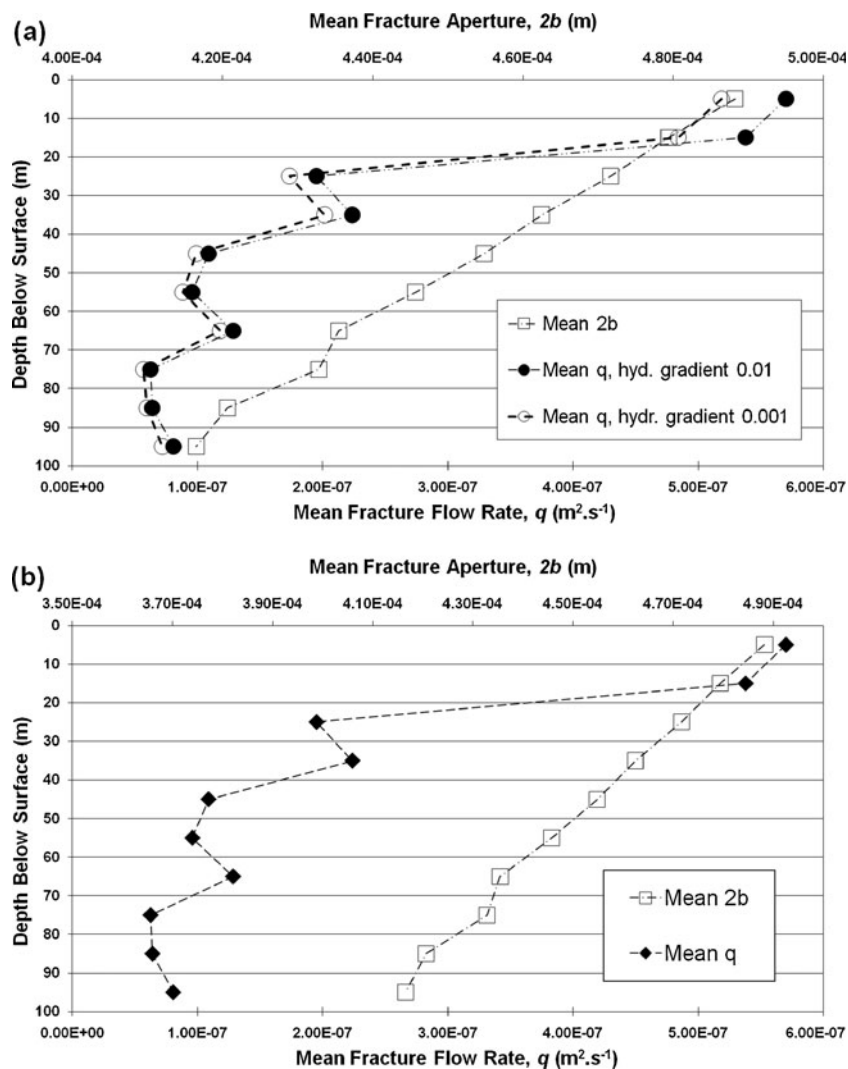


Fig. 11 a UDEC-estimated mean-fracture flow rates (circles, lower x-axis) and fracture apertures (squares, upper x-axis) for the Wendouree NE–SW cross-section model under a normal stress regime. Closed and open circles equal fracture flow rates calculated at hydraulic gradients of 0.01 and 0.001 , respectively. The initial fracture hydraulic apertures were set at 0.5 mm. Reprinted from Mortimer et al. (2011) with permission from Elsevier. b Comparison between UDEC estimated mean fracture flow rates for both the deformed (circles) and undeformed (squares) Wendouree NE–SW cross-section model under a normal stress regime and hydraulic gradient of 0.01 . The initial fracture hydraulic aperture for the deformed model is 0.5 mm, which is fixed at all depths for the undeformed model. Reprinted from Mortimer et al. (2011) with permission from Elsevier

maximum and minimum K directions with the bedding and joint planes is not a function of the 30° model rotations because one of these model rotations/gradient alignments is exactly coincident with the bedding plane direction. The estimated K ellipse at 20 m depth is a relatively smooth oval shape reflecting the overall higher fracture density and permeability of the upper zone of the conceptual model. Commencing from 40 m depth (corresponding to the transition to the deeper, low fracture density zone) the strongly asymmetric shape of the K ellipses (i.e. the high ratio between the maximum and minimum K axes) are reasonably similar reflecting the dominance of the persistent dense bedding planes against a background of decreasing joint set densities.

The overall shape of the hydraulic conductivity ellipses for the deformed models closely mimic those of the undeformed models with the exception that they are slightly

reduced in their absolute magnitudes of K (Fig. 12a–d). For example, compared to the undeformed model, the maximum and minimum K values for the identical but deformed model at 100 m depth are reduced by ~ 10 and $\sim 2.3\%$, respectively. This implies that the shape and magnitude of the hydraulic conductivity ellipses are controlled by the original structure of the fracture network (i.e. fracture geometry and density) and only marginally influenced by the imposed normal stress regime. Furthermore, the magnitude of the UDEC-derived K estimates are in reasonable agreement with those estimated from the pump test derived bulk K_b (see Fig. 6b), particularly, commencing from >40 m depth. However, at shallower depths of between 0 – 40 m, the UDEC models underestimate the magnitude of K by two orders of magnitude compared to the pump test results. The most likely explanation for this difference lies in the true effects of weathering (increased permeability) and the difficulty in

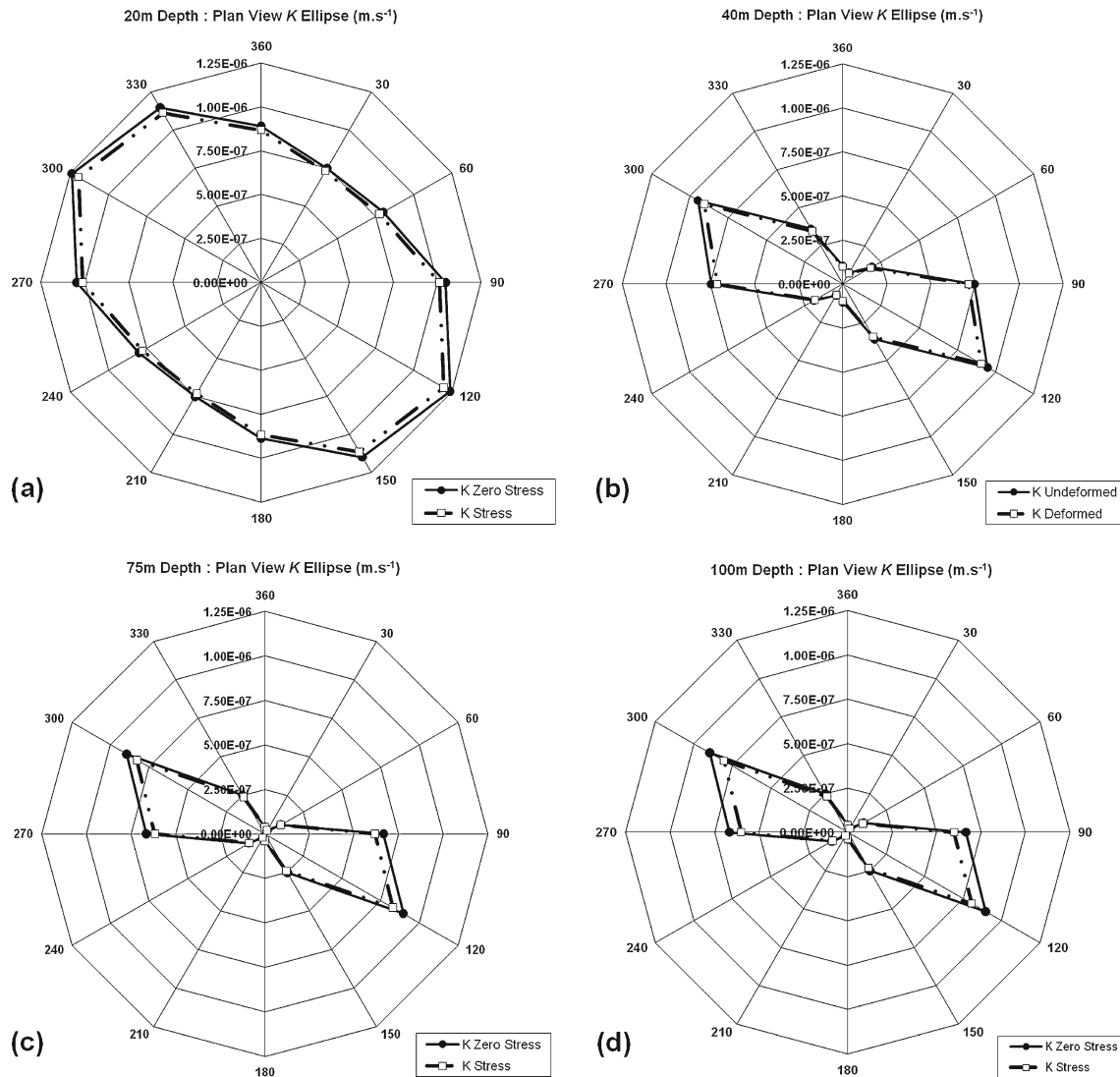


Fig. 12 Undeformed (*solid contour*) versus deformed (*broken contour*) hydraulic conductivity (K) ellipses (m.s^{-1}) for Wendouree at **a** 20 m; **b** 40 m; **c** 75 m and **d** 100 m depth below the surface. Reprinted from Mortimer et al. (2011) with permission from Elsevier

accurately capturing true fracture densities at these shallow depths within the stochastic-based UDEC models. For example, although increased development of unloading-related, sub-vertical flexural and sub-horizontal sheeting (or relaxation) joints closer to the surface is expected, accurately locating and quantifying such features without representative outcrop is difficult.

Small-scale hydraulic connectivity models

This horizontal planar model represents a simple 1×1 m sized snapshot taken from the larger model located at 100 m depth (see Fig. 9c). This model uses identical model parameters to the large-scale models; however, each individual fracture is comprised of segments 0.15 m in length. To demonstrate how fracture network hydraulic connectivity and conductivity can be altered, the results are presented in terms of: (1) the amount of fracture normal closure occurring across the model (i.e. 2b); (2) estimated flow rates for individual deformed versus

undeformed fractures that intersect the eastern and western model boundaries (i.e. q); and (3) a comparison of the sum of discharge flow rates between the deformed and undeformed models (i.e. Q). The flow model methodology is the same as that used to estimate the large-scale K ellipses (see section [Hydraulic conductivity ellipses](#)). That is, under a normal stress regime corresponding to 100 m depth below the surface, initial (and zero stress) hydraulic apertures set at 0.5 mm and steady-state fluid flow under an applied E–W hydraulic gradient of 0.01 with the north and south boundaries acting as impermeable no-flow barriers.

Figure 13 is a plot of fracture normal closure (i.e. aperture closure) that has occurred within each individual fracture of the network, depicting the variable distribution of deformation as dictated by fracture orientation and segment stiffness. The maximum recorded joint closure was 0.116 mm (–23.2%). This plot shows how variable fracture deformation along individual fractures can lead to the development of localised hydraulic restrictions or

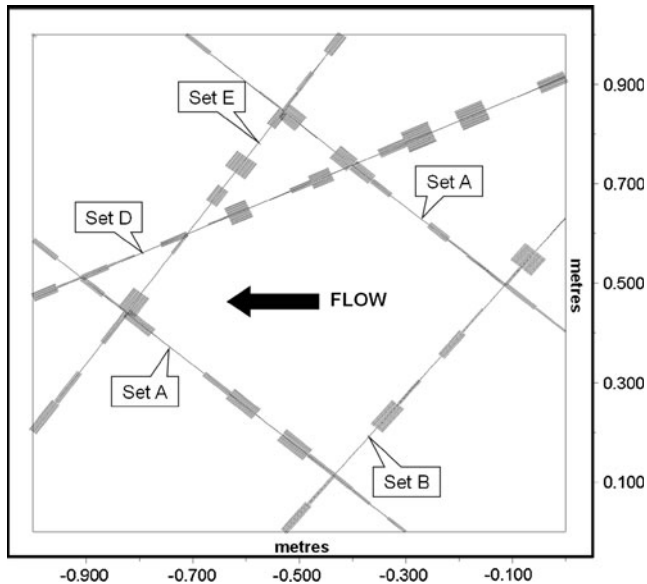


Fig. 13 Plot of modelled fracture normal (aperture) closure that has occurred along each individual fracture of the 1×1 m horizontal planar model located at 100 m depth below the surface (in the plane of set C). The grey shaded patches represent fracture segments that have experienced aperture closure due to fracture deformation with the magnitude of closure represented by the thickness of the patch. Sets B1 and B2 are represented as a single set B as their mean strike orientations are approximately equal. The initial reference (undeformed) aperture for all fractures was 0.5 mm and the two bedding planes (set A) were 0.5 m apart

“chokes” within the flow network, even if the fracture is favourably oriented within the in situ stress field. Figure 14a and b shows a comparison for calculated fracture flow rates for individual fractures that intersect the western (LHS) and eastern (RHS) model boundaries, respectively, for both deformed and undeformed versions of the same model. Figure 14a shows significantly decreased fracture flow rates at the western boundary of the deformed model of between 31–35% when compared to the undeformed model. Similarly at the eastern model boundary, Fig. 14b demonstrates how the network hydraulics and flow is modified by the formation of localised flow-path restrictions due to variable fracture closure. For example, when compared to the undeformed model, the deformed model shows a significant flow restriction in the uppermost fracture intersection (y intercept=0.91 m) which allowed only negligible flow to occur resulting in increased flow occurring in the lowermost fracture (y intercept=0.4 m). In terms of the bulk sum of discharge flow rates occurring at the western (LHS) model boundary, the undeformed versus deformed models recorded 2.4×10^{-6} and $1.61 \times 10^{-6} \text{ m}^3 \cdot \text{s}^{-1}$ respectively. This shows that the variable fracture deformation and resultant hydraulic chokes led to a bulk flow rate decrease of 32.9% consistent with the flow rate reductions experienced by the individual deformed fractures intersecting the western (LHS) boundary. For the first time, the results of these small-scale models support the findings of Shapiro et al. (2007) as well as demonstrate one of the key physical processes involved in the formation of localised “bottlenecks” that

impede groundwater flow and limit the bulk hydraulic conductivity to the least hydraulically conductive interconnected fractures within the network.

Discussion

Long et al. (1982) found that a fractured rock mass will behave like an equivalent porous medium (EPM) if: (1) fracture density is high; (2) apertures are constant and not distributed; (3) orientations are distributed and not constant; and (4) large sample sizes are tested. With respect to hydraulic connectivity, this conclusion by Long et al. (1982) highlights two important points. Firstly, the bulk permeability of a fractured rock aquifer is dependent upon hydraulic connectivity as determined by the distribution of fracture densities, extents, orientations and hydraulic apertures. Secondly, as these fracture properties are inherently heterogeneous within an aquifer, hydraulic connectivity is best evaluated as a bulk property at a large enough scale to be representative of the fractured rock mass. However, identifying the key parameters that dictate fracture network connectivity is complex and needs to be addressed at various scales. This study found that the direct and indirect

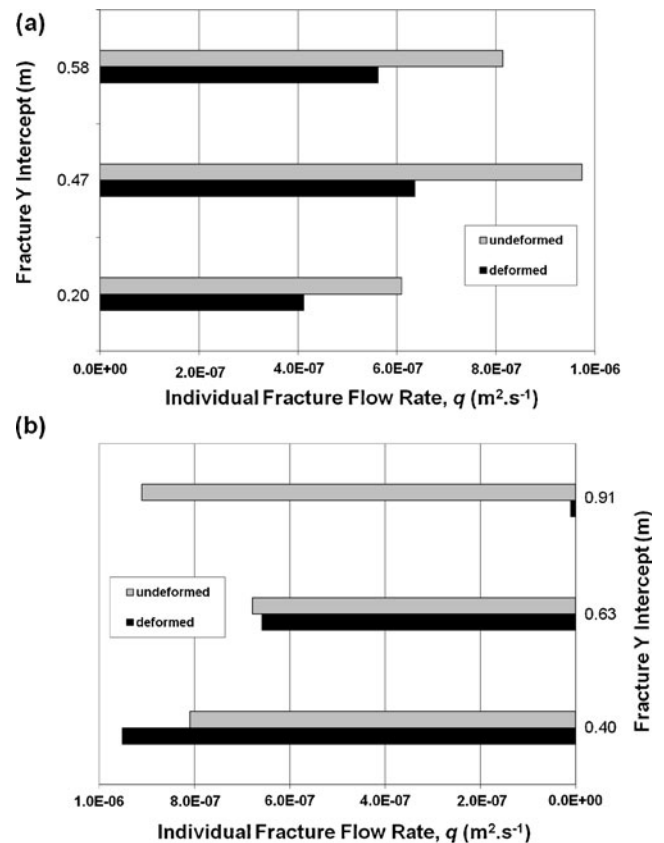


Fig. 14 Bar chart of fracture flow rates (q , $\text{m}^2 \cdot \text{s}^{-1}$) for individual fractures that intersect **a** the western (LHS) model boundary; and **b** the eastern (RHS) model boundary for both the deformed (black) versus undeformed (grey) 1×1 m model. Refer to Fig. 13 for the location of fracture intersections (y intercept) along the eastern and western model boundaries

identification of the key determinants of fracture network connectivity required investigation at scales ranging from sub-metre to >100 metres. Small-scale features include sub-surface fracture deformation, aperture and stiffness distributions as well as methodologies that involve the in situ hydraulic characterisation of individual fractures. Large-scale features include the original structural framework within the host rock sequence, depth-dependent fracture density changes and the effects of the present-day in situ stress field.

A fracture network with constant fracture apertures (i.e. undeformed) has a permeability tensor that is determined by the primary features of the fracture network such as fracture geometry, density, extents, etc. This can be better described as the “inherent permeability” of the fracture network. This study has shown that secondary processes such as the effects of the present-day in situ stress field, weathering and uplift and unloading can fundamentally modify this inherent permeability. These processes result in higher degrees of spatial heterogeneity within shallow groundwater systems by modifying the original distribution of fracture densities and hydraulic apertures. When attempting to characterise this spatial variability, HM models are ideal as they can incorporate natural, depth- and stress-dependent changes in fracture density and aperture. In contrast, standard, non-deforming, discrete fracture network (DFN) modelling techniques typically rely on applying a pre-defined range of estimated fracture hydraulic properties across the fracture network model, which may or not be realistic. The HM models used in this study not only produced results consistent with the field observations but also highlight the strong influence of the in situ stress field in determining the final distribution of sub-surface fracture hydraulic apertures and ultimately hydraulic connectivity. Regardless of the scale, geological setting or nature of the in situ stress field, the physical processes that govern sub-surface fracture deformation and how it can modify the inherent connectivity and permeability of a fracture network is expected to hold true, as in situ stress is ubiquitous. Locally variable fracture closure along the fracture traces results in hydraulic chokes in the 2D models but in 3D this process also incorporates the effects of: (1) increased tortuosity due to normal and shear deformation; and (2) wedging and intense deformation at block corners (fracture intersections) due to block rotations. The latter process may lead to substantial anisotropy in flow patterns at the scales of individual blocks. Thus, when extrapolating the results of 2D models to 3D flow patterns, one needs to consider possible distributions of constrictions in each fracture plane perpendicular to the general flow direction.

There are many techniques available to measure or infer the physical properties of fractures yet despite being directly linked, fracture connectivity remains unquantifiable and difficult to ascertain in the field. Useful methods for detecting hydraulic connection within an aquifer include EM surface and DC surface, borehole-to-surface and cross-borehole surveys, which are relatively less expensive and time consuming than establishing observa-

tion wells or conducting hydraulic pump tests. However, on their own, these particular geophysical surveys have limited practical use due to their individual resolution limitations with both their shallow depths of effective penetration and their ability to define a broad range of conductive fracture orientations. For example, DC borehole-to-surface surveys are more sensitive to steeply dipping conductive fractures, whilst DC cross-borehole surveys are more sensitive to shallow dipping conductive fractures due to the coupling angles involved between the current and potential electrodes (Skinner and Heinson 2004). The accurate interpretation and numerical modelling of these geophysical datasets requires prior knowledge of the structural geology of the study site. In particular, the identification of features that control hydraulic connectivity requires a detailed knowledge of the distribution of all fracture properties, which can only be gained through a multi-disciplinary methodology aimed at characterising the aquifer both structurally and hydraulically. Furthermore, this process would not be complete without knowledge of other regional-scale influences such as the extent of any weathering and the nature of the in situ stress field. Conventional methods for detecting hydraulic connection within an aquifer typically include direct borehole hydraulic tests (e.g. pump, tracers etc), which requires the establishment of multiple wells and is restricted to only a limited number of point source locations. In contrast, this study has shown that spatial variations in aquifer hydraulic connectivity can also be identified through single well datasets such as flow meter and environmental tracer profiles as well as catchment-scale groundwater yield profiles. However, the use of these simpler datasets requires a direct comparison with the known geology and geological setting in order to eliminate them as causative factors.

The stochastic HM models used in this study were designed to capture the key processes at various scales and relate them back to the field observations. For example, the individual fracture set deformation profiles of Fig. 10 shows diverging rates of fracture aperture deformation for each individual fracture set and demonstrates how hydraulic connectivity is progressively modified with increasing depth. The differing rate of deformation for each separate fracture set is a physical process that occurs on a large scale. The greater rate of aperture closure in gently dipping fractures than steeply dipping fractures leads to the progressive restriction of lateral hydraulic connectivity/flow with increasing depth (Fig. 10). This phenomenon was noted during various field studies such as the pump tests and environmental tracer profiles of Love (2003) and the geophysical surveys of Skinner and Heinson (2004). The comparison between the deformed and undeformed flow models (Fig. 11) showed that in situ stress fields do progressively modify groundwater flow patterns similar to that of the field observations which could not be explained by factors such as weathering and/or lithology.

In contrast, the use of the small scale (1×1 m) models was designed to illustrate how localised flow restrictions or

“chokes” form within the fracture network through preferential deformation of locally, low stiffness (i.e. weak) fractures or fracture segments regardless of their geometry, as normal and shear stiffness can vary substantially along a single fracture plane (Fig. 13). This small-scale physical process can explain localised departures from expected fracture deformation and flow trends. The significant modification of network connectivity and reduction in both individual fracture and bulk rock mass flow rates in the deformed versus undeformed small-scale HM models (see Figs. 13 and 14) supports the finding of Shapiro et al. (2007), that bulk hydraulic conductivity is determined by the least hydraulically conductive interconnected fractures in the network. However, based on this finding, Shapiro et al. (2007) inferred that the discrete high K fractures identified within their 3–5 m wide packer-isolated sections of single wells must, therefore, not be connected to the overall fracture network. Our study shows that variable stiffness and resulting restrictions across each fracture plane more convincingly explain why seemingly high K fractures do not proportionally contribute to flow rather than their complete isolation from the network. Importantly, this phenomenon was shown to be a widespread phenomenon.

A notable exception to these findings are the departures from overall fracture flow rate trends observed in the relatively deep, localised, hydraulically active fractures as revealed in the hydro-logging profiles of Love (2003) (see Fig. 6, ~80–85 m). Based upon their occurrence at depths much greater than 40 m below the surface, these particular groundwater-active fractures appear to be stress-insensitive and are most likely locked open as a result of other processes such as earlier fracture deformation episodes (e.g. shear dislocation) or partial mineral infill and cementation (e.g. Banks et al. 1996; Laubach et al. 2004).

The near identical shape and increasing anisotropy of the horizontal planar Wendouree K ellipses with depth for both the deformed and undeformed models, is attributed to the integrated effects of decreasing joint density with depth against a persistent background of dense, through-going bedding planes. As expected, the horizontally isotropic normal stress field ($\sigma_v > \sigma_H = \sigma_h$) had only a minimal effect on the shape of the K ellipses other than a minor reduction in the magnitudes of K . This demonstrates that K ellipses in rock masses with predominant fracture sets are strongly controlled by the original structure of the fracture network (i.e. the inherent permeability). Unlike the vertical cross-section flow model, the stress-related reductions in K with depth associated with the horizontal planar models are approximately linear. This is most likely because these horizontal planar models do not include the sub-horizontal joints of set C, which in turn implies that these sub-horizontal fractures are critical to overall fracture network connectivity. This fact is supported by the Wendouree borehole-to-borehole geophysical surveys of Skinner and Heinson (2004) which detected lateral flow along a small number of extensive low-angle structures becoming more prevalent at depths >30 m. Considering that the sub-horizontal joints are not favourably oriented

(i.e. are preferentially closed) with respect to the in situ normal stress regime, their significant role in governing groundwater flow shows their importance to overall network connectivity.

The use of HM models in this study was successful in demonstrating some of the key physical processes that determine fracture network connectivity and its spatial variability. However, it is important to recognise some of the limitations of this approach, which are largely due to the complexities and uncertainties associated with data capture, sample representativeness and spatial confidence. This is particularly true in relation to the geomechanical characterisation of in situ rock material and fractures such as, for example, the estimation of fracture stiffness, which ultimately dictates fracture deformation behaviour. Generating statistically significant datasets of rock mass and fracture parameters may not always be possible in areas with little to no outcrop or drill core samples. Similarly, model results are dependent on an accurate definition of the prevailing in situ stress field which can vary significantly in regime, orientation and magnitude at shallow depths (Engelder 1993). Without some form of direct or indirect field validation (e.g. in situ stress test, measured anisotropic permeability orientation versus fracture orientation) based on a comprehensive practical knowledge of in situ stress analysis, the choice of in situ stress field should be made considering a range of possibilities so that the model results can bracket the actual conditions. Furthermore, the computational limitations and run time requirements for codes such as UDEC restrict their practical application to either detailed small-scale (<100 m) studies or stochastic representations of larger-scale problems. These HM models can reflect regional-scale patterns if the aquifer is homogeneous at the scale of the REV although numerous HM models may need to be tested at various scales to ascertain what that is. Generally, HM models offer non-unique solutions and as such they require a parameter sensitivity analysis and, if possible, a direct comparison with field-based observations. Nonetheless, this study demonstrated that this HM modelling methodology can produce results that are in good agreement with direct field observations and can offer an alternative preliminary approach to standard borehole hydraulic tests without the need for multiple observation wells.

Conclusion

The identification of the key determinants of fracture network connectivity requires a multi-disciplinary approach that defines the structural and hydraulic character of the fracture network at sub-metre to hundreds of metres scales. Although difficult to quantify, the influence of hydraulic connectivity on groundwater flow is not only evident in conventional multi-well hydraulic tests but also in single well and catchment-scale datasets such as borehole flow meter, environmental tracer and groundwater yield profiles. The field detection and character-

isation of the spatial variability of hydraulic connectivity within a fracture network can also be achieved with electrical and electromagnetic surface and borehole methods. In this study, the use of stochastic HM models at various scales highlighted the significant role of the present-day in situ stress field in determining overall fracture network connectivity and the localised formation of hydraulic chokes, which for the first time quantitatively and qualitatively support the findings of Shapiro et al. (2007).

The key conclusions from this multi-disciplinary study are: (1) the primary control on fracture network connectivity is its inherent permeability as dictated by features such as the distribution of fracture density, orientation, planar dimensions, aperture and roughness; (2) the inherent permeability and connectivity of a fracture network can be modified by secondary processes such as weathering, uplift and unloading and fracture deformation in response to the in situ stress field; (3) heterogeneous fracture deformation results in the formation of hydraulic chokes that impede fluid flow; and (4) the bulk hydraulic conductivity of a fracture network is controlled by the least hydraulically conductive interconnected fractures which imposes a physical limit on the overall hydraulic conductivity of a fractured rock aquifer. The results of the small-scale HM models suggest that this physical limitation on overall bulk rock mass hydraulic conductivity is a widespread phenomenon.

Acknowledgements The authors gratefully acknowledge the funding and logistical support received for this research from the Centre for Groundwater Studies, the Department of Water, Land and Biodiversity Conservation South Australia and the University of Hong Kong. The authors would also like to thank M. Coulthard, J. Ward, S. Chan and M. Christianson for their assistance with the UDEC models, T. Halihan for the use of his geological data and W. Preiss and T. Wilson for additional project support and advice.

References

- Anderson EM (1951) The dynamics of faulting and dyke formation with application to Britain. Oliver and Boyd, Edinburgh
- Bandis SC (1993) Engineering properties and characterization of rock discontinuities. In: Hudson J (ed) *Comprehensive rock engineering: principles, practice and project*, vol 1, chap 6. Pergamon, Oxford, UK, pp 155–183
- Banks D, Odling NE, Skarphagen H, Rhor-Torp E (1996) Permeability and stress in crystalline rocks. *Terra Rev* 8:223–235
- Barton CA, Zoback MD, Moos D (1995) Fluid flow along potentially active faults in crystalline rock. *Geology* 23:683–686
- Barton NR, Choubey V (1977) The shear strength of rock joints in theory and practice. *Rock Mech* 10(1–2):1–54
- Barton N, Bandis S, Bakhtar K (1985) Strength, deformation and conductivity coupling of rock joints. *Int J Rock Mech Min Sci Geomech Abs* 22(3):121–140
- Bour O, Davy P (1998) Connectivity of random fault networks following a power law length distribution. *Water Resour Res* 33:1567–1583
- Cappa F, Guglielmi Y, Fenart P, Merrien-Souketchoff V, Thoravel A (2005) Hydromechanical interactions in a fractured carbonate reservoir inferred from hydraulic and mechanical measurements. *Int J Rock Mech Min Sci* 42:287–306
- Cook PG, CSIRO Land and Water (2003) A guide to regional groundwater flow in fractured rock aquifers. Seaview, Payneham, Australia, 108 pp
- Cook PG, Love AJ, Robinson N, Simmons CT (2005) Groundwater ages in fractured rock aquifers. *J Hydrol* 308:285–301
- Davy P, Bour O, De Dreuzy J-R, Darcel C (2006) Flow in multi-scale fractal fracture networks. In: Cello G, Malamud BD (eds) *Fractal analysis for natural hazards*. Geological Society, London, pp 31–45
- de Dreuzy J-R, Davy P, Bour (2001) Hydraulic properties of two-dimensional random fracture networks following a power law length distribution: 2. permeability of networks based on log-normal distribution of apertures. *Water Resour Res* 37(8):2079–2095
- Engelder T (1985) Loading paths to joint propagation during a tectonic cycle: an example from the Appalachian Plateau, U.S. *A. J Struct Geol* 7(3/4):459–476
- Engelder T (1993) *Stress regimes in the lithosphere*. Princeton University Press, Princeton, NJ, 457 pp
- Gaffney ES, Damjanac B, Valentine GA (2007) Localization of volcanic activity: 2. effects of pre-existing structure. *Earth Planet Sci Lett* 263:323–338
- Ge S (1998) Estimation of groundwater velocity in localised fracture zones from well temperature profiles. *J Volcan Geotherm Res* 84:93–101
- Geological Survey of South Australia (2001) South Australia geoscientific GIS dataset. Division of Minerals and Energy Resources, PIRSA, Adelaide, Australia
- Hancock PL, Engelder T (1989) Neotectonic joints. *Geol Soc Am Bull* 101:1197–1208
- Hillis RR, Reynolds D (2000) The Australian stress map. *J Geol Soc* 157:915–921
- Hoek E (2007) *Practical rock engineering*. <http://www.rocksience.com/hoek/PracticalRockEngineering.asp>. Cited May 2008
- Hsieh PA (1998) Scale effects in fluid flow through fractured geologic media. In: Sposito G (ed) *Scale dependence and scale independence in hydrology*. Cambridge University Press, Cambridge, UK, pp 59–66
- Itasca (2004) UDEC 4.0 theory and background. Itasca, Minneapolis, MN
- Kulhawy FH, Goodman RE (1980) Design of foundations on discontinuous rock. *Proceedings of the International Conference on Structural Foundations on Rock*. *Int Soc Rock Mech* 1:209–220
- Laubach SE, Olsen JE, Gale JFW (2004) Are open fractures necessarily aligned with the maximum horizontal stress? *Earth Planet Sci Lett* 222:191–195
- Long JC, Witherspoon PA (1985) The relationship of the degree of interconnection to permeability in fracture networks. *J Geophys Res* 90(B4):3087–3098
- Long JC, Remer JS, Wilson CR, Witherspoon PA (1982) Porous media equivalents of discontinuous fractures. *Water Resour Res* 18(3):645–658
- Love AJ (2003) Groundwater flow and solute transport dynamics in a fractured rock meta-sedimentary aquifer. PhD Thesis, Flinders University, South Australia, Australia
- Love AJ, Cook PG, Harrington GA, Simmons CT (2002) Groundwater flow in the Clare Valley. Report DWR02.03.0002, Department for Water Resources, Adelaide, Australia
- Love AJ, Simmons CT, Cook P, Herczeg A, Halihan T (2007) Estimating groundwater flow rates in fractured rock metasediments: Clare Valley, South Australia. In: Krasny J, Sharp JM Jr (eds) *Groundwater in fractured rocks*. IAH Selected Paper Series vol 9, IAH, Goring, UK, pp 463–478
- Min KB, Jing L, Stephansson O (2004) Determining the equivalent permeability tensor for fractured rock masses using a stochastic REV approach: method and application to the field data from Sellafeld, UK. *Hydrogeol J* 12:497–510
- Mortimer L, Aydin A, Simmons CT, Love AJ (2011) Is in situ stress important to groundwater flow in shallow fractured rock aquifers? *J Hydrol* 399(3–4):185–200
- National Research Council (NRC) (1996) *Rock fractures and fluid flow: contemporary understanding and applications*. National Academy of Sciences, Washington, DC

- Nordlund E, Radberg G, Jing L (1995) Determination of failure modes in jointed pillars by numerical modelling. In: *Fractured and jointed rock masses*. Balkema, Rotterdam, The Netherlands, pp 345–350
- Odling NE, Gillespie P, Bourguin B, Castaing C, Chiles J-P, Christensen NP, Fillion E, Genter A, Olsen C, Thrane L, Trice L, Aarseth E, Walsh JJ, Watterson J (1997) Variations in fracture system geometry and their implications for fluid flow in fractured hydrocarbon reservoirs. *Petrol Geosci* 5:373–384
- Paillet FL (1993) Using borehole geophysics and cross-borehole flow testing to define hydraulic connections between fracture zones in bedrock aquifers. *J Appl Geophys* 30:261–279
- PIRSA (2009) Drillhole enquiry system. Online database, PIRSA, Adelaide, Australia. <https://des.pir.sa.gov.au/deshome.html>. Cited January 2009
- PIRSA Minerals (1999) Earthquakes in South Australia > Magnitude 3, 1995–1999. Online report, PIRSA, Adelaide, Australia. http://www.pir.sa.gov.au/minerals/earthquakes/yearly_earthquake_reports. Cited May 2006
- PIRSA Minerals (2001) Earthquakes in South Australia 2001. Online report, PIRSA, Adelaide, Australia. http://www.pir.sa.gov.au/minerals/earthquakes/yearly_earthquake_reports. Cited May 2006
- Preiss WV (1995) Tectonic evolution of the mid-north, South Australia. In: *Specialist Group in Tectonics and Structural Geology, Clare Valley mid-conference excursion guide*. Geol Soc Aust Abs 40
- Preiss WV (2000) The Adelaide Geosyncline of South Australia, and its significance in continental reconstruction. *Precamb Res* 100:21–63
- Price NJ (1966) *Fault and joint development in brittle and semi-brittle rock*. Pergamon, Oxford, UK
- Renshaw CE (1996) Influence of subcritical fracture growth on the connectivity of fracture networks. *Water Resour Res* 32(6):1519–1530
- Renshaw CE (1999) Connectivity of joint networks with power law length distributions. *Water Resour Res* 35(9):2661–2670
- Renshaw CE (2000) Fracture spatial density and the anisotropic connectivity of fracture networks. In: *Faybishenko, B, Witherspoon, PA, Benson SM (eds) Dynamics of fluids in fractured rocks*. AGU Geophysical Monograph 122, AGU, Washington, DC, pp 169–184
- Rutqvist J, Stephansson O (2003) The role of hydromechanical coupling in fractured rock engineering. *Hydrogeol J* 11:7–40
- Sandiford M (2003) Neotectonics of southeastern Australia: linking the Quaternary faulting record with seismicity and in situ stress. In: *Hillis RR, Muller D (eds) Evolution and dynamics of the Australian Plate*. Geological Society of Australia, Spec. Publ. 22, GSA, Sydney, pp 107–120
- Sandiford M, Wallace M, Coblenz DD (2004) Origin of the in situ stress field of southeastern Australia. *Basin Res* 16:325–338
- Skinner D, Heinson G (2004) A comparison of electrical and electromagnetic methods for the detection of hydraulic pathways in a fractured rock aquifer, Clare Valley, South Australia. *Hydrogeol J* 12:576–590
- Shapiro AM, Hsieh PA, Burton WC, Walsh GJ (2007) Integrated multi-scale characterization of ground-water flow and chemical transport in fractured crystalline rock at the Mirror Lake site, New Hampshire. In: *Hyndman DW, Day-Lewis FD, Singha K (eds) Sub-surface hydrology: data integration for properties and processes*. AGU Geophysical Monograph Series 171, AGU, Washington, DC, pp201–225
- Snow DT (1969) Anisotropic permeability of fractured media. *Water Resour Res* 5(6):1273–1289
- Van der Pluijm BA, Marshak S (2004) *Earth structure: an introduction to structural geology and tectonics*. Norton, New York, 656 pp
- Waltham T (2002) *Foundations of engineering geology*, 2nd edn. Taylor and Francis, London
- Wellman TP, Poeter EP (2006) Evaluating uncertainty in predicting spatially variable representative elementary scales in fractured aquifers, with application to Turkey Creek Basin, Colorado. *Water Resour Res* 42. doi:10.1029/2005WR004431
- Zhang X, Sanderson DJ (1996) Numerical modelling of the effects of fault slip on fluid flow around extensional faults. *J Struct Geol* 18:109–119
- Zhang X, Sanderson DJ, Harkness RM, Last NC (1996) Evaluation of the 2-D permeability tensor for fractured rock masses. *Int J Rock Mech Min Sci Geomech Abs* 33:17–37
- Zoback MD (2007) *Reservoir geomechanics*. Cambridge University Press, New York